# Optimal Design and Operation of an Off-grid Hybrid Renewable Energy System in Nigeria's Rural Area, Using Fuzzy Logic and Optimization Techniques

Afolabi, Oladayo Taofeek
九州大学総合理工学府環境エネルギー工学専攻

# Optimal Design and Operation of an Off-grid Hybrid Renewable Energy System in Nigeria's Rural Area, Using Fuzzy Logic and Optimization Techniques

**TAOFEEK AFOLABI**

Supervisor
**Associate Professor. Hooman Farzaneh**

**February 2023**

Energy and Environmental Systems Laboratory,
Department of Energy and Environmental
Engineering Interdisciplinary Graduate School of
Engineering Sciences

**KYUSHU UNIVERSITY**
**Japan**

# Table of Contents

# List of Figures

# List of Tables

# ABSTRACT

Over half of the Nigerian population is not connected to the grid, and those who are connected to the grid only have about 7 hours of electricity per day and experience 10 blackouts each week. As a result, most businesses and individuals resort to alternative energy sources such as gasoline or diesel generators to meet their daily energy needs. Nigeria currently has an entire installed capacity of 12.5GW, out of which only around 3GW gets to the end users. For Nigeria to meet up with its proposed "Electricity Vision 30:30:30", which goal is to generate 30GW of electricity by the year 2030 with renewables providing more than 30% of the energy mix, the techno-economic analysis of the renewable energy potential of Nigeria needs to be assessed and established.

Nigeria is blessed with numerous renewable energy sources, which can be harnessed to provide energy to the country. With Nigeria's high insolation, solar energy has been adjudged as one of the best ways to generate electricity in the country. Solar energy is clean, easy to install, and relatively cheaper. However, with Nigeria's grid infrastructure deficiency which causes losses on the grid, solar energy is best consumed where it is produced, to provide power for the numerous Nigerians that live off the grid.

This research, therefore, focuses on the technical and economic analysis of implementing an off-grid Hybrid Renewable Energy System (HRES) in a community situated in Ogun state, Nigeria, as a case study. The contribution made by this paper in the quest to determine the optimal design and operation of a stand-alone hybrid renewable energy system (HRES) which is supposed to be deployed in a rural community called "Olooji" in Nigeria are two folds: First, a size optimization model is developed based on the novel metaheuristic Particle Swarm Optimization (PSO) technique to find the optimal configuration of the proposed off-grid system based on the minimization of the Levelized Cost of Electricity, taking into account the local meteorological and electricity load data and details technical specification of the main components of the HRES. Second, a Fuzzy Logic Controlled Energy Management System (EMS) will be developed for dynamic power control and energy storage of the proposed HRES, ensuring the optimal energy balance between the different multiple energy sources and the load at each hour of the operation.

The result of the size optimization model showed that an LCOE for implementing an HRES in the community would be 0.48 USD/kWh in a full battery capacity scenario. However, due to the high capital cost associated with this full battery capacity scenario, a second scenario with half of the battery capacity was considered, and an LCOE of 1.17 USD/kWh was realized. The high value of LCOE for the second scenario is due to the high cost of diesel fuel.

The result from this study is important for quick decision-making and effective feasibility studies for optimal techno-economic synopsis of implementing mini-grids in rural communities. This will help increase HRES execution, reduce electricity costs, and ensure electricity availability in rural communities in Nigeria.

**Keywords:** Hybrid Renewable Energy system (HRES), Particle Swarm Optimization (PSO), Fuzzy Logic Control (FLC), Energy Management System (EMS), Loss of Power Supply Probability (LPSP), Levelized Cost of Energy (LCOE), Microgrid

# ACKNOWLEDGMENT

I thank Almighty Allah, the Lord of everything that exists, for his mercies and guidance over me and more specifically, for seeing me through the completion of my master's program.

My sincere appreciation goes to my supervisor, Associate Professor Hooman Farzaneh, for his persistent support, guidance, and efforts throughout my master's program at Kyushu University. His untiring efforts and mentorship instilled discipline, diligence, and time management in me, enabling me to prioritize my work schedules. The weekly meetings with him helped a lot in formulating my research direction. The monthly presentation helped fine-tune my presentation skills and subject my research progress to the radar of all laboratory members for criticism and evaluation. All these endeavors built my confidence in the process of performing research, presenting progress, and publishing results.

My appreciation also goes to all my colleagues at Energy and Environmental Science (EES) laboratory from different countries and backgrounds with whom we interacted, shared experiences, and worked together under one roof. Our interactions made me see unity in human diversity. Without you all, the laboratory experience would not have been sweeter.

I would like to appreciate the African Development Bank (AfDB) and every member of the Japan African Dream Scholarship (JADS), without whom my journey into this academic program would not have started. The scholarship offered by AfDB through JADS provided me with financial resources that allowed me to gain knowledge in such a developed society as Japan. This experience upgraded my academic qualification and improved my international exposure. I was able to observe first-hand the advanced technologies in Japan and experienced Japanese culture in a way that was peaceful to my heart. I would also acknowledge the JADS-support team of the International Development Center of Japan (IDCJ) for their support.

I would also like to appreciate ACOB LIGHTING TECHNOLOGY LIMITED, where I worked before coming to Japan, working with ACOB helped in acquiring data for my case study.

My appreciation goes to my family for their endless love and support. To my mother and my uncles, for their endless love and moral support over the years, and to all whom I would not be able to mention their names due to the constraints of space and time.

THANK YOU to you all.

Taofeek Afolabi, Kyushu University, Chikushi Campus, Fukuoka, Japan
February 2022.

# Chapter 1

# INTRODUCTION

## 1.1 Current Electricity Situation in Nigeria

Nigeria, the most populous country in Africa, has one of the lowest rates of electrification in the world [1]. About 43% of the Nigerian population, representing 85 million people, have no access to grid electricity [2]. Nigerian households connected to the grid have electricity only for about 7 hours a day and experience more than 10 blackouts every week, with most people running diesel or gasoline generators for more than 4 hours a day [3]. Those who receive electricity from the grid experience more than 17 hours of blackout daily. Therefore, most households and businesses resort to self-electricity generation using alternative sources such as diesel or gasoline generators.

Nigeria's national grid is currently being managed by the Nigeria Electricity Regulatory Commission (NERC), which is responsible for formulating policies and regulating the power sector, and the Power Holding Company of Nigeria (PHCN), which is accountable for coordinating investments and operations of the power sector. The duos were created in 2005 after the National Electric Power Authority (NEPA) was decoupled when the Electric Power Sector Reform Act (EPSRA) was enacted for the privatization of the power sector [4]. PHCN is currently being grouped into three divisions which include generation companies (GENCOS), a transmission company (TRACO), and eleven (11) distribution companies (DISCOS). The GENCOS consists of more than fifty (50) Independent Power Producers (IPPs), ten (10) National Integrated Power Projects (NIPPs), and six (6) privatized PHCN, which include Afam, Egbin, Kainji, Sapele, Shiroro, and Ughelli Power Plc; the TRACO is the Transmission Company of Nigeria (TCN) while the eleven (11) DISCOS include Abuja Electricity Distribution Company, Benin Electricity Distribution Company, Ibadan Electricity Distribution Company, Eko Electricity Distribution Company, Enugu Electricity Distribution Company, Ikeja Electricity Distribution Company, Jos Electricity Distribution Company, Kaduna Electricity Distribution Company, Port Harcourt Electricity Distribution Company, Kano Electricity Distribution Company, and Yola Electricity Distribution Company [5]. The GENCOS are responsible for producing electricity, the TRACO is responsible for transmitting electricity from the GENCOS to the DISCOS, while the DISCOS are responsible for distributing electricity to the final consumers.

The present entire installed capacity of the GENCOS is around 12.5GW, out of which 5.4GW is inaccessible and 3.3GW is non-functional, remaining just around 3.9GW of electricity the GENCOS can functionally produce and dispatched to the TRACO; 0.3GW is lost while transmitting to the DISCOS, leaving around 3.6GW the DISCOS can distribute to the final consumers; 0.5GW is lost during distribution and just about 3.1GW gets to the final consumers [6][7]. Figure 1.1 shows the Nigeria Power Sector energy flow in megawatts (MW). Nigeria's daily electricity need is approximately 8GW to 17GW, although, estimating Nigerians' electricity need is complicated by the passive demand due to unavailable electricity [1]. Considering the

Nigerian population of over 200 million people [8] and a rule of thumb estimates of 1GW for a million people [7], Nigeria will only get the electricity needed to support full industrialization when the country can produce up to 200GW of electricity. According to the World Bank, Nigeria's electricity consumption stands at 144.52 kWh per capita compared to over 5,500 kWh per capita in European countries [9].

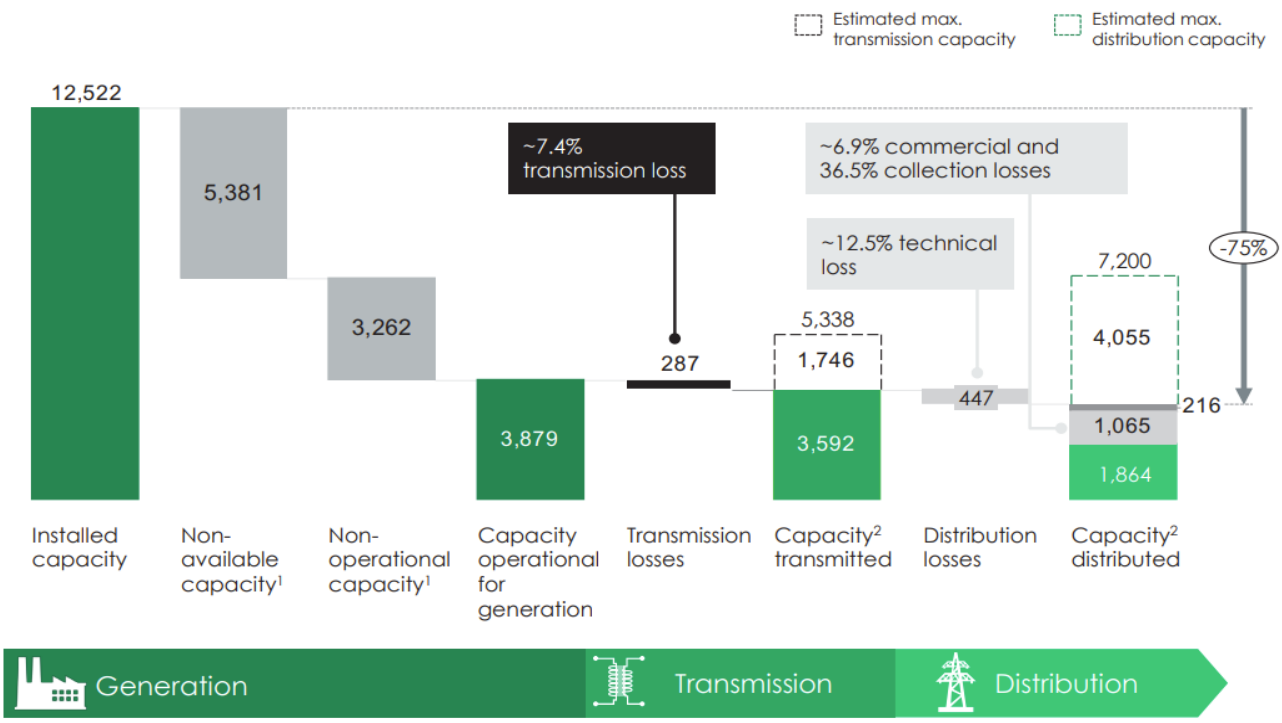


Figure 1.1: Nigeria Power Sector Energy Flow. Adopted from [6]

The quoted data shows that Nigeria's current generation capacity is far below the population demand. This imbalance between the electricity generated and the demand creates an epileptic and unreliable electricity situation in the country. Furthermore, the data shows that just around 25% of the entire installed capacity reaches the final consumer; this is partially connected to the disturbances in gas supply, because most electricity producing plants are gas-fueled. In fact, eighty-five percent of the entire installed capacity is by gas-fueled thermal power plants, and the remaining 15% is by hydroelectric power plants [6]. Therefore, to meet Nigeria's electricity demand, generating energy using fossil fuels is not advisable due to their severe environmental and health impacts. It is, therefore, important to assess the renewable energy potential for electricity generation in Nigeria.

### 1.2 Renewable Energy Potential for Nigeria's Electrification

In recent times, renewable energy has become a panacea to energy problems worldwide because it is clean, environment-friendly, and ultimately cheaper. Nigeria has a massive capacity for generating electricity from its numerous green energy resources, with a daily energy potential of

934 GWh from Biomass, 120 GWh from solar, 84 GWh from hydro, and 44 GWh from wind [10]. Nigeria's photovoltaic power output potential (kWh/kWp) is shown in Figure 1.2, while the wind speed available in each Nigeria state is shown in the Nigeria Wind Resource Map in Figure 1.3.,

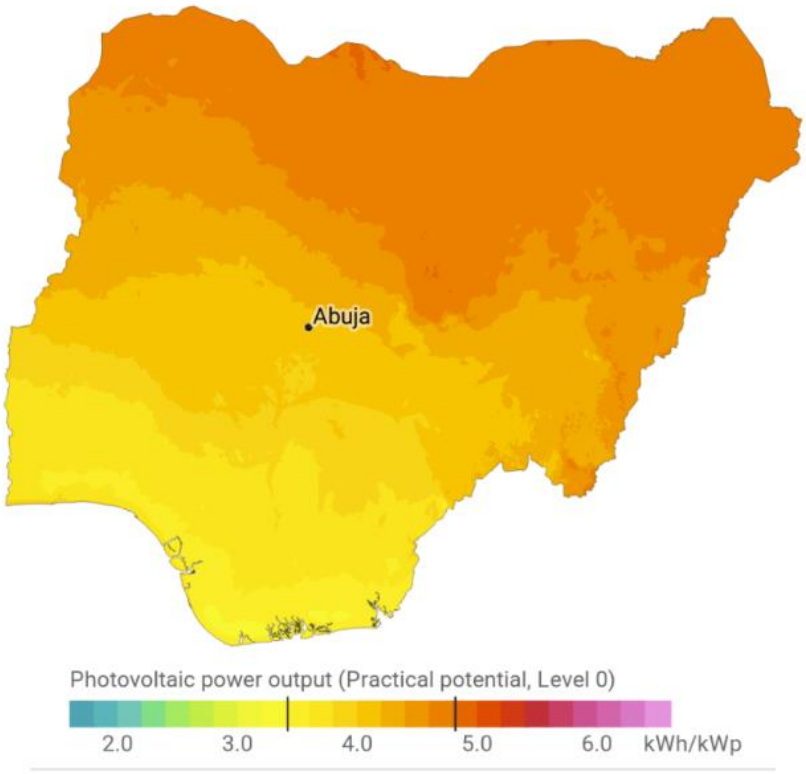


Figure 1.2: Nigeria Photovoltaic power output potential [11]

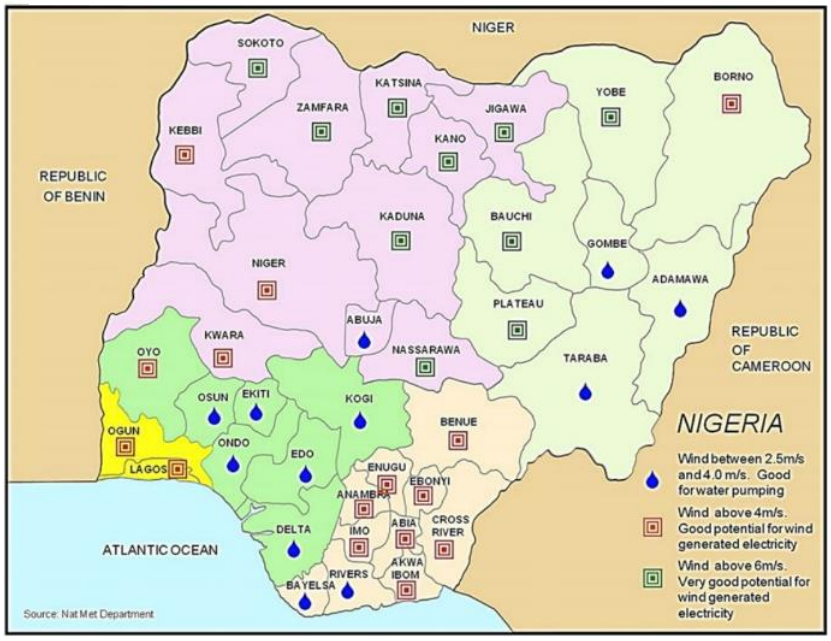


Figure 1.3: Wind Resource Map of Nigeria. Adopted from [12]

Stears data reported that even though there are many potential renewable energy solutions obtainable in Nigeria, solar energy is the best for providing electricity for off-grid areas in Nigeria because of its sufficiency, relatively low-cost, and different strata available for different levels of consumers [1].

Additionally, electricity generated in off-grid regions is best consumed where they are generated. Dispatching the produced electricity to the national grid will only cause more losses and uncertainty in transmission to the end users. Nigeria's transmission grid critically restricts the proportion of the produced electricity that reaches the final consumers. Outworn and ineffective equipment, deficient framework, and insufficient investment in extending the grid makes accessing electricity through the grid ineffective in the long term [1]. It is thus essential to investigate ways off-grid electricity can be positioned to supplement the void in the electricity supply. Shaaban and Petinrin pointed out that exploiting off-grid green energy potentials in Nigeria could reduce the persistent electricity crisis in the country [13].

This research, therefore, focuses on the techno-economic study of implementing an off-grid Hybrid Renewable Energy System in Nigeria and proposes an EMS that ensures the reliability of the HRES operation. It uses a community situated in the southwestern part of Nigeria as a case study.

### 1.3 Motivation

Recently, there has been a proliferation in the adoption of renewable energy systems for generating electricity. Renewable energy accounts for about twenty percent of global final energy consumption, with the most significant growth occurring in the electricity sector. Global capacity increased by more than eight percent in 2013 [14]. During these periods, the main drivers of the global energy market were solid economic growth and continued population growth in developing countries [15]. This is due to the advocacy by governments and international organizations for the supply of renewable energy to remote regions that are off the grid and to reduce the world's environmental impact and greenhouse effects exacerbated by non-renewable energy production and consumption. These developments have increased efforts to establish renewable energy plants in many nations worldwide to access more sustainable energy and combat environmental degradation and climate change issues [15].

However, the usage of these renewable energy systems is usually in hybrid form as the availability of all renewable energy sources is not dependable. A hybrid renewable energy system (HRES) integrates many renewable technologies and operates as an independent power system with higher reliability than a single renewable energy source [16]. Because renewable energy is sourced from the natural environment, it is dependent on weather conditions, which makes it difficult to get stable electricity systems using renewable sources [17]. The two most important renewable energy sources for off-grid distributed energy systems, wind, and photovoltaic (PV) sources, are affected by random fluctuations due to their dependence on short-term weather and seasonal climate variations [18].

Hybrid Renewable Energy System (HRES) is becoming more defined as a micro-grid or

decentralized generation (DG) that consists of two or more renewable energy sources such as solar PVs, wind turbines, fuel cells, and other renewable energy sources working together with other decentralized non-renewable power generation units in a coordinated manner to meet the demand of a particular area [19]. Storage systems such as batteries or hydrogen fuel cells and emergency generation equipment such as a diesel generator are always included in the hybrid renewable energy systems to back up against fluctuation and to ensure reliance. Energy storage equipment stores excess energy, which is released when renewable energy is not available, thereby solving the fluctuation problems associated with renewable energy sources [20], while a diesel generator (DG) is added as an emergency power source to improve HRES reliability [21].

However, the addition of these different units to an energy supply system makes the system more complex both in terms of technological adaptability and economic sustainability. In addition, the operating characteristics and costs of HRES are much higher than those of standalone wind turbines or solar PV systems [22]. This, therefore, calls for designing a cost-effective HRES and an efficient energy management system (EMS) that ensures economic sustainability and technical adaptability for the hybrid system; such a system would ensure optimal operation cost and energy system reliability by reducing the system's LPSP.

### 1.4 Literature Review

Due to several numbers of equipment involved in HRES, excessive sizing leads to exorbitant capital, and insufficient sizing leads to an unreliable system. The two situations are unwanted; therefore, optimal sizing is important when planning HRES. There have been numerous studies on sizing models for HRES, with each of them using either economic indicator (such as Net Present Value (NPV), Levelized Cost of Electricity (LCOE), Total Annual Cost (TAC), Cost of Electricity (COE)), reliability indicators (such as Deficiency of Power Supply Probability (DPSP), Loss of Load Probability (LOLP), Loss of Power Supply Probability (LPSP)), environmental indicators (such as Life Cycle Emission (LCE), Carbon Footprint of Energy (CFOE), Life Cycle Assessment (LCA),) or social indicators (such as social acceptance (SA), Job Creation Index (JCI), Human Development Index (HDI),) as its objective indexes for evaluating the HRES performance. Most existing studies prioritize economic and/or reliability as objective indexes; 43.5% of the surveyed papers consider economic indexes, and 37% consider both economic and reliability indexes as objective indexes [23]. This means that over 80% of the surveyed publications on HRES sizing consider economics and reliability indexes for evaluating their HRES performance.

HRES sizing majorly includes conventional strategies (such as analytical method, numerical method, iterative method, and probabilistic method), Artificial Intelligence (AI) techniques (such as Particle Swarm Optimization (PSO), Cuckoo Search Algorithm (CSA), Genetic Algorithm (GA), Ant Colony Optimization (ACO), Artificial Bee Colony (ABC) and Grey Wolve Optimization (GWO)), hybrid methods (such as GA-ABC, Simulated Annealing-Tabulated Search (SA-TS) and Divide and Conquer-Remote Electrical Tilt (DP-RET)), and computer software (such as Hybrid Optimization Model for Electric Renewables (HOMER), General Algebraic Modeling System (GAMS), Transient System Simulation Tool (TRNSYS), Hybrid Optimization

by Genetic Algorithm (HOGA), LINGO, and HYBRIDS) [23]. Analogous to conventional strategies, AI methods deal with intricate and non-linear problems, while dealing with incomplete data and fluctuating wind and solar energy problems [24]. Among the AI strategies, PSO and GA have higher use cases. GA and PSO constitute more than 50% of the use cases of all AI strategies [23]. Although GA is used more than PSO, PSO is appreciated for its ease of implementation, high accuracy, simple computation, fast convergence, absence of crossover, and lack of mutation operations present in GA [24] [25].

This research considers the use of the PSO because of its advantages over other methods. Many HRES optimization studies use PSO to optimize the power generated by HRES to meet the electrical needs of a typical home and minimize LCOE [26]. Yoshida et al. designed an optimal stand-alone microgrid system consisting of the wind, PV, battery, and diesel generator based on the PSO method to find the optimal system configuration using the lowest cost perspective approach [27]. Mohammed et al. developed a PSO model to optimize the power generated by an HRES, which consists of a wind turbine, tidal turbine, solar PV, and batteries [28]. The designed system was to serve and minimize the energy cost of a stand-alone community in Bretagne, France.

Furthermore, there have been several studies on developing an Energy Management System (EMS) to ensure energy balance for HRES. Currently, most of the EMS-related research of HRES is on distributed energy systems in microgrids and electric vehicles [29]. EMS strategies can be categorized into intelligence-based controls, such as Wavelet Neural Network (WNN), machine learning, and multi-objective optimization methods; rule-based controls, such as logic threshold and Fuzzy Logic Control (FLC) methods or optimal-based controls, such as instantaneous optimization and global optimization [29].

Of the methods, fuzzy logic control is considered important because its rules are easy to implement and do not involve complex mathematical modeling [29]. Abdullahi and Majed showed the necessity of strengthening an HRES by having at least two kinds of energy storage systems and two kinds of renewable sources for system stability and designed an FLC for the energy management of HRES having multiple types of storage [30]. However, the designed FLC cannot be applied to a more complex system involving a larger distribution network, as in the case of microgrids.

In a study comparing the techno-economic analysis of Solar Home System (SHS) and microgrids to determine the best choice for rural electrification, Chaurey and Kandpal found that microgrid is a more economical option for providing power to an off-grid community with more than 500 densely populated households [31]. The techno-economic analysis of a microgrid investigated by Borhanazad through the design of a stand-alone off-grid hybrid PV/wind/diesel/battery system for a rural community in Malaysia showed that having 56-61% of solar energy inclusion is important to achieve an optimal and economically feasible hybrid system [32]. To minimize the power demand of buildings in Japan, Tatsuya et al. used a fuzzy logic controller to design a grid-tied hybrid solar/wind/hydrogen system with a maximum power point tracker (MPPT) and got a 2% excess power generation from the designed HRES [33]. Berrazouane proposed a Cuckoo Search Algorithm-tuned FLC to operate an autonomous hybrid power system

and discovered that the optimized FLC could reduce the LPSP, LCOE, and excess energy of the systems [34].

Table 1.1: Summary of Literature Survey on HRES

| Country | Research Goal | System Components | Objective Function | Optimization method | Impact Category | Ref. |
|---|---|---|---|---|---|---|
| Japan | To design an optimal stand-alone microgrid for powering a residential area. | PV/wind/battery /DG | Total cost | PSO | Economic | [27] |
| France | To optimize the power generated by a hybrid renewable energy system | Wind turbine/Tidal turbine/PV module/Battery | Total Net Present Cost | PSO | Economic | [28] |
| Australia | To control the power flow of an HRES with multiple renewable energy sources and multiple energy storage systems | PV/Wind/Fuel cell/Battery | EMS control | Fuzzy Logic | Reliability | [30] |
| India | To make a techno-economic comparison between SHS and microgrid | SHS/ PV-wind-battery-DG | Annualized life cycle costs (ALCC) | Homer | Economic | [31] |
| Malaysia | To investigate the techno-economic analysis of an optimal standalone HRES in remote areas. | PV/wind/battery /DG | COE LPSP | PSO | Economic, Reliability | [32] |
| Japan | To reduce the load demand of buildings on HRES. | Grid-tied hybrid solar–wind–hydrogen | LCOE | Fuzzy Logic | Economic | [33] |
| Algeria | To develop an optimal FLC for operating a stand-alone HRES based on CSA. | PV/battery/DG | LPSP, Excess Energy, LEC | Fuzzy Logic | Economic, Reliability | [34] |

### 1.5 Research Gap and Research Contribution

Optimal sizing and control are two distinct aspects of the same HRES system. A system that is optimally sized but not optimally controlled will be inefficient. Optimal sizing ensures minimal implementation cost and energy affordability, while optimal control ensures optimal operation cost and energy availability. The literature survey showed that most of the research papers only focus on system sizing or energy control. However, the size, cost, control, and reliability of HRES are all interdependent; an effective energy management system needs to be integrated with an

appropriate sizing method. This research aims to develop an optimal sizing model that finds the least cost configuration of the HRES system, which is then integrated into an EMS model that ensures optimal energy scheduling during HRES operation in an off-grid community. Integration of the two systems will produce a combined model that ensures energy reliance at the optimal cost. The study uses PSO to find the equipment sizing that gives the best cost at optimal reliability and uses a Fuzzy Logic Controller to design an EMS that ensures energy balance between the energy demand and the energy supply every time during the HRES operation.

### 1.6 Thesis Organization

This study uses the PSO strategy and the FLC method to develop models for optimal sizing and optimal control of HRES. Chapter 2 introduces the size optimization model, the structure of the HRES, and the mathematical modeling of the constituent components of the HRES. Chapter 3 presents the design of an optimal Fuzzy Logic Controlled Energy Management System. Chapter 4 shows the characteristics of the case study community, the renewable energy resource data, the load data, the economic data and the technical parameters of the equipment. Simulation results are presented and discussed in chapter 5. Finally, the achievement of the research objectives is acknowledged in chapter 6, the concluding chapter.

# Chapter 2

# Size Optimization Model

## 2.1 System structure

Figure 2.1 shows the typical structure of the considered HRES. The system contains two renewable energy sources, solar photovoltaic modules, and a wind turbine. The battery is included as a backup power source, while the diesel generator serves as an emergency supply. An inverter is included that converts direct current to alternating current and vice-versa. The consumer load is the energy demand of the community. The inverter is assumed to contain an energy management system that controls the power flow between the load demand and the different energy sources. The mathematical modeling of each component is shown below.

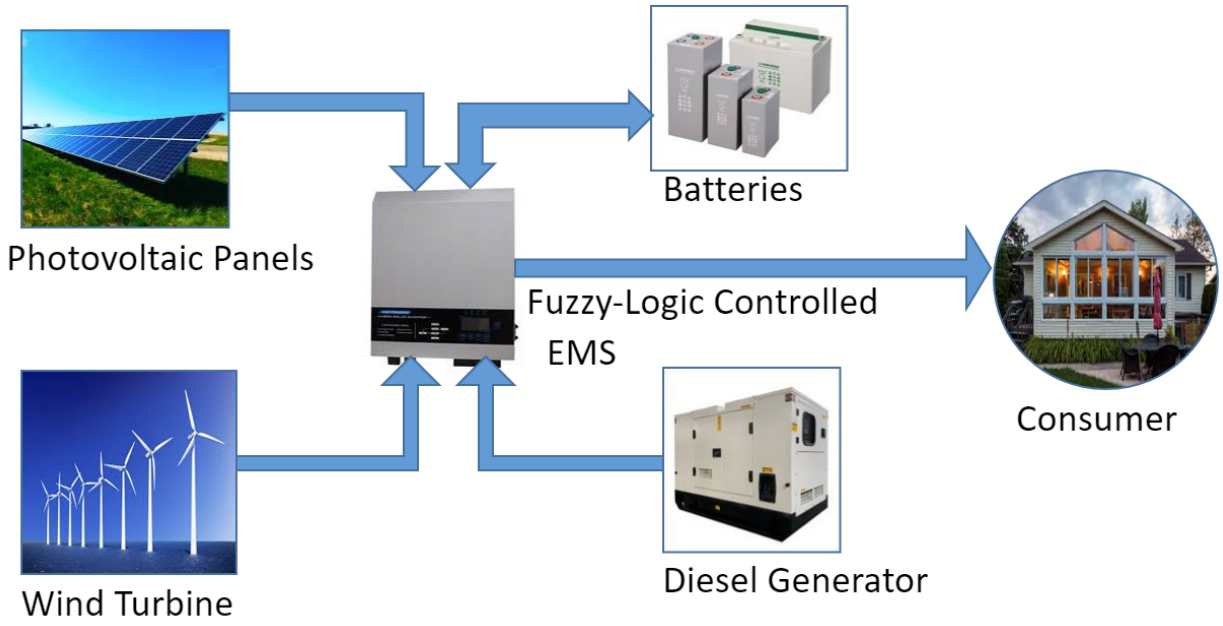


Figure 2.1: Hybrid renewable energy system structure

## 2.2 Solar PV model

Solar PV output power is influenced by factors such as solar irradiance, yearly season, the surrounding temperature, the type of PV module, and the inclination angle. The solar panel output power $P_{PV}$ is determined by a simplified simulation model and is given by following the equations [28]

$$P_{PV} = N_{PV} \times \eta_{PV} \times A_m \times G_t \quad (2\text{-}1)$$

$$\eta_{PV} = \eta_{ref} \times \eta_{pc}[1 - \beta(T_c - T_{cref})] \quad (2\text{-}2)$$

$$T_c = T_a + \left(\frac{NOCT-20}{800}\right) \times G_t \quad (2\text{-}3)$$

Where $T_{a.NOCT} = 20℃\ and\ G_{t,NOCT} = \frac{800W}{m^2}$ for the wind speed of 1m/s. $N_{PV}$ is the number of PV panels, $\eta_{PV}$ is the panel efficiency, $A_m$ is the total area of the panel module and $G_t$ is the incident global irradiance (W/m$^2$ ), $T_a$ is the surrounding temperature, $NOCT$ is the normal PV working temperature (℃).

### 2.3 Wind turbine model

The power output of a wind turbine is determined by the regional wind speed and wind turbine characteristics. This study used the following equations to determine the output power of a wind turbine [27]:

$$P_w(V) = \begin{cases} \frac{p_r(V - V_{CIN}))}{V_{rat} - V_{CIN}} . V_{CIN} \le V \le V_{rat} \\ P_r .\ V_{rat} \le V \le V_{CO} \\ 0,\ V \le V_{CIN} and\ V \ge V_{CO} \end{cases} \quad (2\text{-}4)$$

$$V = V_{ref}\left(\frac{H}{H_{ref}}\right)^{\alpha} \quad (2\text{-}5)$$

Where $H_{ref}(m)$ is the reference height, $V_{ref}(m/s)$ is the reference height's wind speed, $\alpha$ refers to the exponent; $H(m)$ is the height of the wind turbine, V is the wind speed at $H(m)$, and $V_{rat}\ (m/s)$ is the rated wind speed of the wind turbine, $P_r(kW)$, is the constant power, $V_{CIN}\ (m/s)$ is the cut-in speed and $V_{CO}(m/s)$ is the cut-out speed.

### 2.4 Battery model

Battery stores electrical energy in chemical form. Energy stored in the battery is used to power the load when renewable energy is not sufficient. The battery capacity is estimated by the following equation [32].

$$C_B = \frac{E_L . S_D}{V_B . DOD_{\_\max} T_{cf} . \mu_B} \quad (2\text{-}6)$$

Where $V_B$ is the battery working voltage, $E_L$ is the load in Wh; $T_{cf}$ is the temperature correction factor, $S_D$ is the autonomy days, $DOD_{max}$ the depth of discharge; and $\mu_B$ is efficiency.

Also, the battery SOC is defined as the available capacity divided by the rated capacity of the battery in Ampere Hours (AHr). This is mathematically expressed below [32].

$$SOC = \frac{Available\ Capacity(AHr)}{Rated\ Capacity(AHr)} \times 100 \quad (2\text{-}7)$$

$$SOC(t) = SOC(t-1).(1-\sigma) + \left[E_{Gen(t)} - \frac{E_L(t)}{\mu_{inv}}\right]\mu_B \quad (2\text{-}8)$$

$$SOC(t) = SOC(t-1).(1-\sigma) + \left[\frac{E_L(t)}{\mu_{inv}} = E_{Gen(t)}\right]\mu_B \quad (2\text{-}9)$$

$$State\ of\ Charge = 1 - Depth\ of\ Discharge \quad (2\text{-}10)$$

Where $E_L$ is load, $\sigma$ is the self-discharge rate an hour, and $E_{Gen}$ is the energy generated, Eq(2-8) is for the battery charging, while Eq(2-9) is for the battery discharging. The battery operates optimally between the allowable discharge limit denoted as $SOC_{low}$ and the allowable maximum charge limit denoted as $SOC_{max}$.

## 2.5 Power Flow Strategy

For the optimal sizing of the HRES system using the PSO, the power flow needs to be balanced such that renewable energy is optimally utilized while ensuring that energy is always available to power the load. The HRES considered in this study comprises of: the PV, wind turbine, battery, DG, and load. The power management for the PSO ensures that there is a balance between the energy supplied and the energy demanded. At every hourly timestep, the PSO program compares the renewable energy (solar and wind) with the load and then decides whether to charge the battery, discharge the battery, or start the diesel generator depending on the conditions. When the energy supplied by renewable energy (RE) is enough to power the load, the excess energy is used to charge the battery. When the RE is not enough to power the load and the battery SOC is greater than the lowest SOC, energy is taken from the battery to power the load. When the RE is insufficient to power the load, and the battery SOC is lower than the lowest SOC, the diesel generator is switched on to power the load, and the diesel generator's excess energy is used to charge the battery. The flow chart of the power flow strategy is shown in Figure 2.2 below.

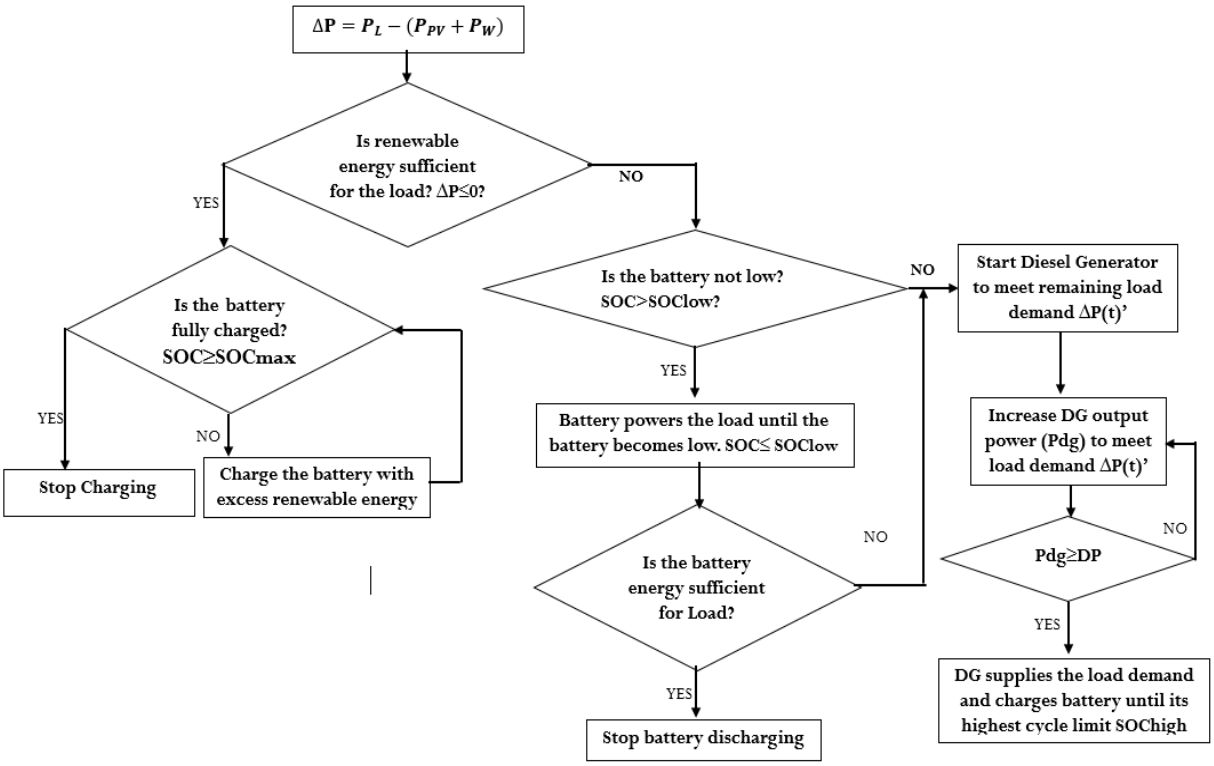


Figure 2.2: Power Flow Strategies for the PSO optimization

## 2.6 Operating Cost of HRES system

The battery replacement cost and the diesel generator running cost constitute the main operating costs of the considered HRES system because other sources only have capital costs with little or no maintenance cost.

### 2.6.1 Replacement Cost of Batteries

The cost of replacing batteries majorly contributes to the overall operating cost of HRES. Battery replacement depends on the battery usage cycle $N_T$, which in turn is dependent on the depth of discharge (DOD). The operating cost of the battery in ($/kWh) is given by ([22]).

$$C_{Bat} = \frac{\sum_{j=0}^{N_T} C_j}{\sum_{j=0}^{N_T} |\Delta P_{batj}|} \quad (2\text{-}11)$$

Where $N_T$ refers to the battery cycle during the operating period. $\Delta P_{batj}$is the battery power output during operating hour j. And $C_j$, the life cost of the battery is given by

$$C_j = \frac{C_{initial-bat}}{N_C} \quad (2\text{-}12)$$

$C_{initial-bat}$ refers to the battery purchase price.

### 2.6.2 Operation cost of the diesel generator

In an HRES, a generator provides the energy needed to power the load at a critical time when renewable energy and battery energy are not enough. A generator needs to be run between 70% and 89% of its rated capacity for optimal efficiency [35]. The fuel consumption of a diesel generator is mathematically expressed as [36]

$$D_f(t) = \propto_D P_{DG}(t) + \beta_D \times P_{Dr} \quad (2\text{-}13)$$

Where $D_f(t)\ in\ (Liter/hour)$ refers to fuel consumption, $P_{DG}(t)\ in\ (kW)$ refers to the DG power generation, $P_{Dr}\ in\ k(W)$ refers to the rated power, $\propto_D$and $\beta_D$ refer to the fuel consumption curve coefficients, which are taken as 0.2461 l/kWh and 0.08415 L/kWh [36]. Fuel cost is given as follows:

$$C_g = \frac{D_f(t)C_f}{P_{DG}} = C_f\left(\propto_D + \frac{\beta_D \times P_{Dr}}{P_{DG}}\right) \quad (2\text{-}14)$$

The DG depreciation cost is given as follows:

$$C_{DW} = \frac{\frac{M_T}{20000} C\_initial_{DG}}{\sum_{t=0}^{M_T} P_{DG}(t)} \quad (2\text{-}15)$$

Where $M_T$ refers to the DG's operating hours during, and $C_{initial_{DG}}$ refers to the DG cost of purchase.

$$C_{DG} = C_g + C_{DW} \quad (2\text{-}16)$$

## 2.7 Particle Swarm Optimization (PSO) Model

Kennedy and Eberhart 1995 proposed the particle swarm optimization algorithm [37]. PSO is a stochastic optimization algorithm based on the population of particles. It has been successfully used in many applications such as face detection, voice recognition, and neural network training because it computes in parallel with fast computing speed. PSO mimics the characteristics of a flock of birds called a "swarm" with a single and possible bird called a "particle," which is the solution. The fitness value for each solution is evaluated for every particle using the fitness function. A velocity vector is also evaluated for each particle. Every solution is updated for each particle in the search space. Each solution is compared over several iterations with the particle's previous and neighbor's positions to determine the optimum value [38]. To reach the optimal point. Each particle updates its position in search space according to its own previous experience and that of its neighbors over iterations. The movement of the particle depends on its present velocity and every element j of the velocity vector of the kth particle is expressed as:

$$V_i^{(k+1)} = \omega \times V_i^{(k)} + C_1 \times rand_1(\cdot) \times P_{best,i} - X_i^{(k)} + C_2 \times rand_2(\cdot) \times (G_{best} - X_i^{(k)}) \quad (2\text{-}17)$$

$$X_i^{(k+1)} = X_i^{(k)} \; V_i^{(k+1)} \quad (2\text{-}18)$$

Where $X_i^{(k+1)}$refers to the new position of $ith$ particle, $V_i^{(k+1)}$ refers to the new velocity vector of $ith$ particle, $rand_1(\cdot)$) and $rand_2(\cdot)$ are random numbers, each within [0,1] ، $C_1$ and $C_2$ refer to the learning factors, ω is the momentum weight factor. $P_{best,i}$ is the prior best experience of $ith$ particle that is recorded and $G_{best}$ refers to the best particle of the entire population.

To arrive at the optimal values for the HRES equipment, the PSO algorithm is used to determine the optimal sizes of the HRES equipment by minimizing the cost (LCOE) function:

$$LCOE\ \left(\$/_{kWh}\right) = \frac{Annualized\ Cost(\$)}{Annual\ Energy\ Supplied\ (kWh)} \quad (2\text{-}19)$$

$$= \frac{Total\ Net\ Present\ Cost(NPC)\ (\$)}{P_{load}(kW)(8760\ \frac{h}{year})} \times Capital\ Revovery\ Factor\ (CRF) \quad (2\text{-}20)$$

$$CRF = \frac{i(i+1)^n}{(1+i)^n - 1} \quad (2\text{-}21)$$

Where $n$ is the project life (24 years), $i$ is the prevailing interest rate, $NPC$ comprises all capital costs, $P_{load}(kW)$ includes all energy supplied in one year. The cost function is subjected to technical and reliability constraints. The reliability constraint (LPSP) is defined as:

$$LPSP = \frac{\sum P_{load} - P_{pv} - P_{wind} - P_{\text{battery}} - P_{DG}}{\sum P_{load}}$$

Where $P_{pv}$ is the PV power, $P_{wind}$ is the wind power, $P_{DG}$ is the Diesel Generator power and $P_{\text{battery}}$ is the usable energy of the battery. The LPSP is to be less than 0.2%. Kashefi et al. stated that an LPSP of less than 1% is acceptable for off-grid electricity supplies as compared to an LPSP

of less than 0.01%, which is accepted in developed countries [39].

The renewable energy resource data which include solar irradiation data, wind data, and temperature data; the equipment characteristics and load consumption data of the community are used to determine the optimum value for the equipment. The load is preferably powered using renewable energy (RE), and power is drawn from the battery only when renewable energy is insufficient. The system uses a diesel generator for emergency supply when the RE is unavailable, and the battery energy is inadequate for the demand. Three separate codes were written to find the LCOE, as detailed in Table 2.1 below. Primarily, MATLAB codes were developed for the technical analysis, the economic analysis, and the Particle Swarm Optimization algorithm. These codes were linked and used to determine the optimal sizing for the HRES equipment considering the renewable energy resource data and the economic data. The input data comprises the equipment cost, equipment parameters, load data, irradiation data, wind speed data, and temperature data of the Olooji community.

The developed PSO codes were run for January (Dry season) and August (rainy season), representing the two seasons in Nigeria. The codes were run in the MATLAB environment at several iterations to evaluate the LCOE while keeping the LPSP at a maximum of 0.2%. Two scenarios were considered. In the first scenario, the boundary conditions used were expanded to allow the algorithm to choose the equipment values without restrictions. In the second scenario, the boundary conditions were restricted to limit the battery size to realistically and economically obtainable. The LCOE, LPSP, PV, wind turbine, DG, and battery values were obtained and recorded for each scenario. The flow chart of the PSO algorithm is shown in Figure 2.3

.

Table 2.1: Procedures for finding the LCOE using PSO Algorithm

| | |
|---|---|
| Technical Analysis | The solar irradiation data, temperature data, wind speed data, consumption data, and equipment characteristics were used to determine the solar panel's output power, the wind turbine's output power, the battery capacity, and the output power of the diesel generator. |
| Economic Analysis | The cost per kilowatt-hour of each component was inputted to determine the capital cost of the HRES. Twenty percent of the capital was budgeted for the yearly operation and maintenance of the HRES. The prevailing interest rate and the prevailing diesel fuel cost in Nigeria were used for the economic analysis. The capital recovery factor was considered to find the net present cost of the HRES. |
| PSO Algorithm | The PSO algorithm considered was constrained to select PV size within [0:150kW], wind turbine size within [0:100kW], battery capacity size within [0:2000kWh], diesel generator size within [0:100kW], and termination criteria included choosing the population to be 5 and the number of iterations to be 100. The algorithm used the meteorological, technical, and economic data information to output the LCOE, LPSP, optimal PV size, optimal wind turbine size, optimal battery capacity, optimal diesel generator, and SOC of the HRES. |

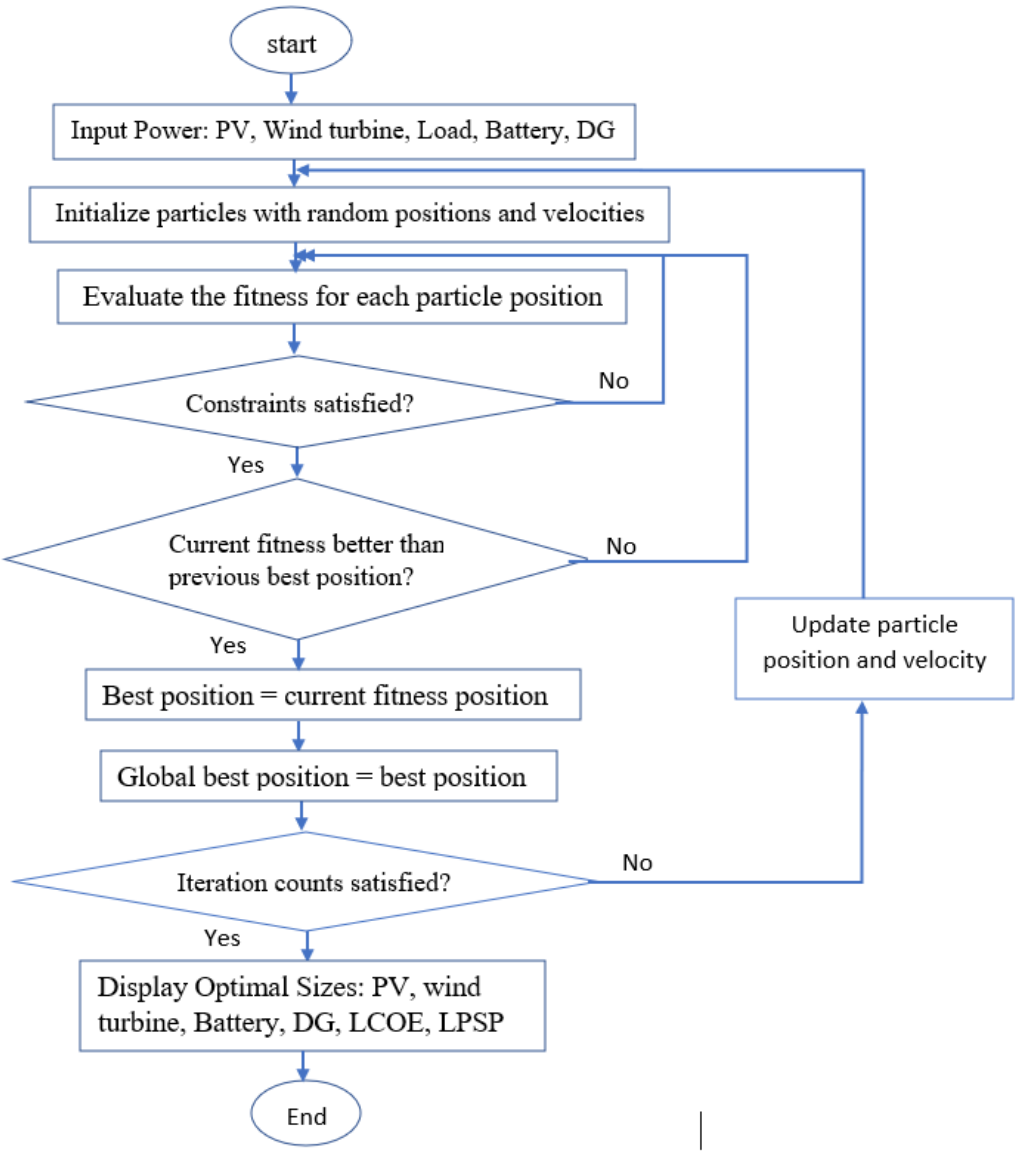


Figure 2.3: Flow chart of the Particle Swarm Optimization (PSO) Algorithm

# Chapter 3

# Optimal Energy Management System using a Fuzzy Logic Controller

Fuzzy logic control is established on multi-valued logic that allows using common principles and expert knowledge for control rules [40]. Its control method is like the human reasoning methods. L. A. Zadeh pioneered the idea of Fuzzy Logic in 1965 [41] and it has since been developed and adapted for different systems to provide effective and efficient control in many applications. Zadeh defined a fuzzy set as a collection of objects with varying grades of membership identified by a membership function that allocates a scale of membership ranging from zero to one to every object [41]. Fuzzy logic control involves the application of fuzzy sets and theories in control processes. The fuzzy logic control method uses range-to-range or range-to-point strategies, unlike the classical control method, which uses point-to-point control. The fuzzy system (Figure 3.1) comprises four units: the fuzzification unit, knowledge unit, intelligence unit, and defuzzification unit. Inputs are converted into fuzzy input by assigning the associated membership functions to the imprecise inputs at the fuzzification unit. The intelligence and knowledge units worked on the fuzzy inputs and inferred proper results by considering the rules to produce a fuzzy output converted back to crisp output at the defuzzification unit [42][30]. The fuzzy logic controller is efficiently employed for energy management control due to its simple and effective feature adaptability to the non-linearity of HRES energy supply and demand [34].

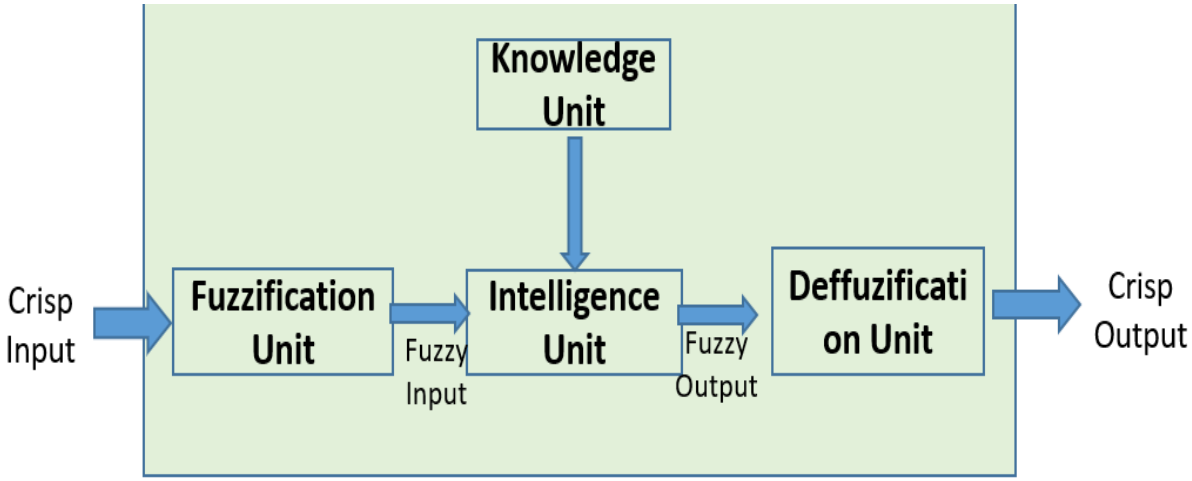


Figure 3.1: Fuzzy Logic Control structure

### 3.1 Design of the Energy Management System

The main function of the energy management system in an HRES is to control the energy flow from each energy source to the load. An optimal energy management system will ensure an energy balance between the demand and the supply and guarantee maximum utilization of the available renewable energy. At every point during the HRES operation, the EMS works to ensure that the power flow satisfies the energy balance between the components, as shown in the equation below:

$$P_{pv}(t) + P_w(t) + P_{batt_{discharge}}(t) + P_{DG}(t) = P_l(t) + P_{batt\_charge}(t) \quad (3\text{-}1)$$

In the EMS considered, the PV power ($P_{pv}$) and wind power ($P_w$) are renewable energy (RE) power. The load is preferably powered using renewable energy (RE), and power is drawn from the battery only when renewable energy is insufficient. The system considers using a diesel generator for emergency supply when the RE is unavailable, and the energy available on the battery is inadequate for the demand, or the battery has depleted to its minimum allowable state of charge (SOC). The differential power ($\Delta P$) is the power difference between the load power ($P_L$) and renewable energy (RE):

$$\Delta P = P_L(t) - (P_{pv}(t) + P_w(t)) \quad (3\text{-}2)$$

The battery State of Charge (SOC) for the FLC is modeled using the SOC equation presented by [22] and given as:

$$SOC\ (t) = \frac{P_{batt}(t-1) + C_{batt}[P_{RE}(t) - P_L(t)] + \{P_{DG}(t) - (1 - C_{batt})[P_L(t) - P_{RE}(t)]\}}{P_{batt}} \quad (3\text{-}3)$$

Where, $P_{batt}(t-1)$ is the remaining energy on the battery in the last hour. The term $C_{batt}[P_{RE}(t) - P_L(t)]$ refer to the current RE charging power or load discharging power and $\{P_{DG}(t) - (1 - C_{batt})[P_L(t) - P_{RE}(t)]\}$ indicatates the current generator charging power, $P_{batt}$ is the battery-rated capacity. If the renewable energy power (RE) is sufficient for the load, ( $\Delta P \leq 0$), and the battery is fully charged ($\mathrm{SOC} \geq \mathrm{SOC_{max}}$), then the battery stops charging. If the renewable energy power $\Delta P$ is sufficient for the load ($\Delta P \leq 0$), but the battery is not fully charged ( $\mathrm{SOC} < \mathrm{SOC_{max}}$), the excesss renewable energy charges the battery until the battery is charged to the maximum ( $\mathrm{SOC_{max}}$). If the renewable energy power $\Delta P$ is insufficient for the load ($\Delta P > 0$) and the battery is charged ($\mathrm{SOC} > \mathrm{SOC_{low}}$), then the battery discharges to power the load until the battery becomes ($\mathrm{SOC} \leq \mathrm{SOC_{low}}$), if the battery energy is sufficient for the load, then the battery stops discharging. If the battery energy is insufficient for the load or the battery is low ($\mathrm{SOC} \leq \mathrm{SOC_{low}}$), then the diesel generator starts to meet the remaining load demand ($\Delta P'$), the DG output power adjusts to meet the remaining load demand until the diesel generator output power ($P_{dg} \geq \Delta P'$). The DG supplies the load demand and charges the battery until the battery is fully charged ($\mathrm{SOC} \geq \mathrm{SOC_{max}}$). Figure 3.2 shows the flow chart of the energy management system considered in this study.

For efficient and optimal power control, the fuzzy logic controller was designed to schedule among the energy sources and establish the energy balance of both the supply and demand sides. The solar irradiation data, the wind data, the equipment sizing obtained from the PSO optimization model (discussed in chapter 2), and the load consumption data of the Olooji community were considered, to analyze the performance and effectiveness of the fuzzy logic controller. The Fuzzy Logic Controlled Energy Management System (FLC-EMS) was designed in MATLAB Simulink IDE. The hybrid renewable energy system was first designed using the optimal sizes of the equipment obtained from the optimal sizing model, the power demand, the solar irradiance, and the wind speed data of the community.

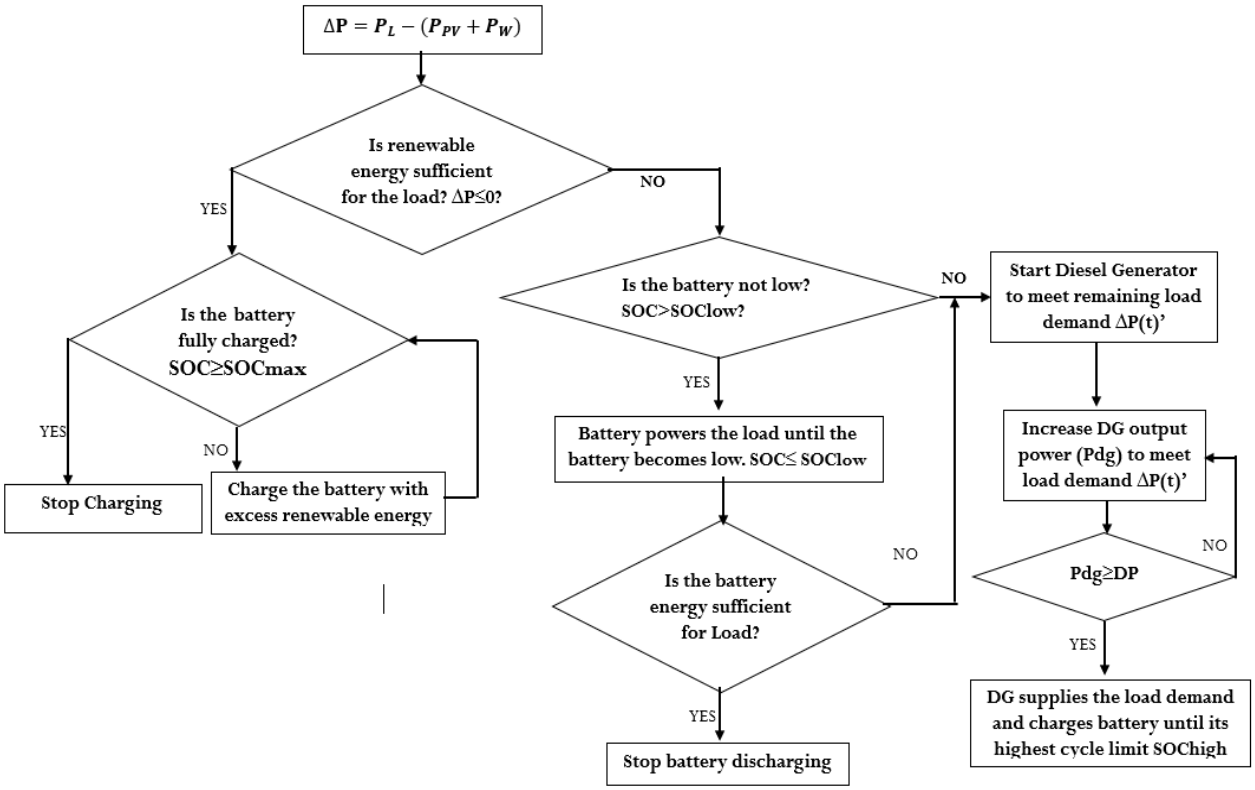


Figure 3.2: Flowchart of the energy allocation processes.

Figure 3.3 shows the interconnection between the designed HRES and the designed FLC Energy Management System. The solar power, wind power, load power, and battery power signals from the HRES are used as inputs into the FLC Energy Management System. This study uses two FLC controllers denoted as FLC1 and FLC2. Figure 3.4 below shows the HRES simulation diagram.

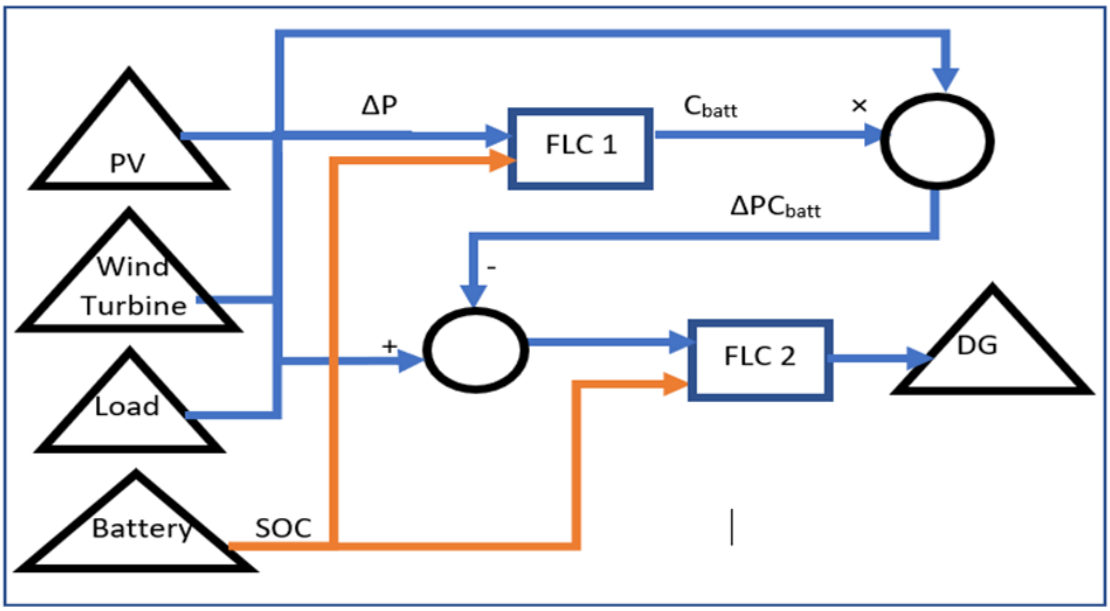


Figure 3.3: The signal flow of the Fuzzy Logic Controllers

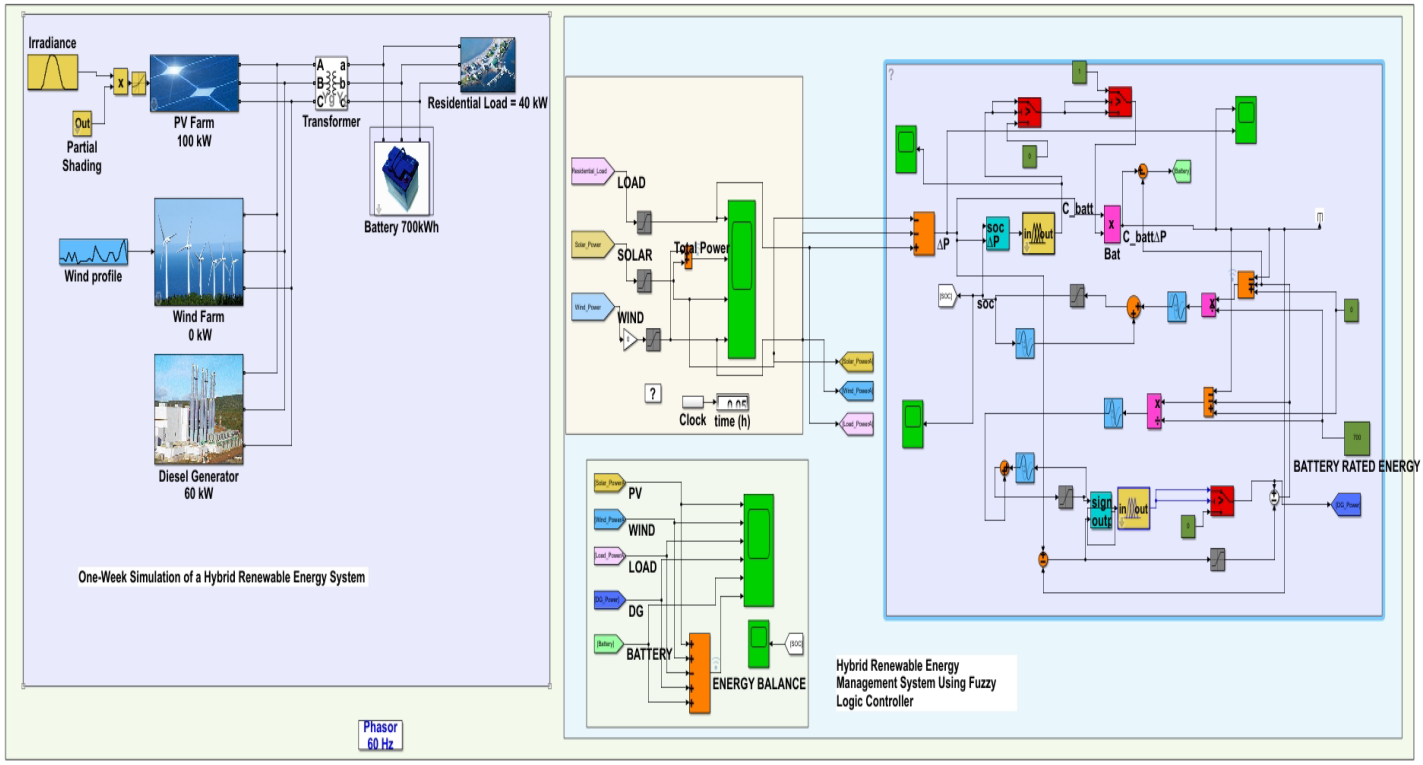


Figure 3.4: The designed HRES and FLC in MATLAB Simulink IDE

The fuzzy logic controllers operate based on the strategies discussed in Section 3.1. Tables 3.5 and 3.6 show the control rules to be implemented by FLC1 and FLC2, respectively. These rules are based on the operator's/expert's knowledge. For membership functions, 'V' represents 'Very,' 'L' represents 'Low,' 'H' represents 'High,' 'S' represents 'Standard', 'M' represents 'Much', 'P' represents 'Positive', 'N' represents 'Negative'. Battery SOC, the input 1 to the FLC1, has a universe of discourse running from 0 to 1 with seven (7) variables. The differential power (ΔP), the input 2 to the FLC1, has its universe of discourse running from -80kW to 60kW and has six (6) variables. The two inputs produce a total of forty-two (42) fuzzy logic rules. The battery multiplier constant, $C_{batt}$ , which is the output of FLC1, has its universe of discourse runs from 0 to 1. The $C_{batt}$ membership function also has seven (7) variables. The membership function for each variable is plotted as shown in Figure 3.5. Battery SOC (t-1) which is the input 1 to the FLC2, has its universe of discourse runs from 0 to 1 with seven (7) variables, and the excess power, ΔP, which is the input 2 to the FLC2, has its universe of discourse runs from -80kW to 40kW with nine (9) variables. The two variables give rise to a total of sixty-three (63) fuzzy logic rules. The diesel generator output power, $P_{DG}$, which is the output of FLC2, has its universe of discourse runs from 0 to 50kW with eight (8) variables. The membership functions of the variables are plotted as shown in Figure 3.6.

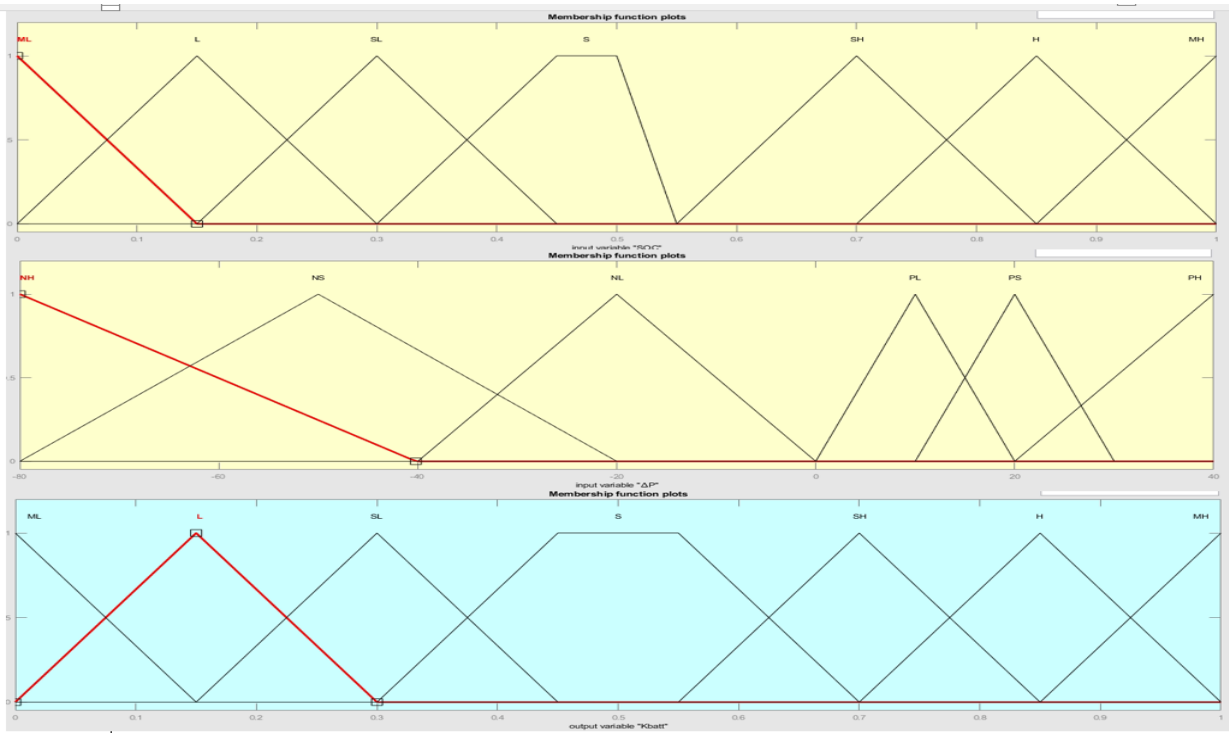


Figure 3.5: The membership functions of the FLC1 variables

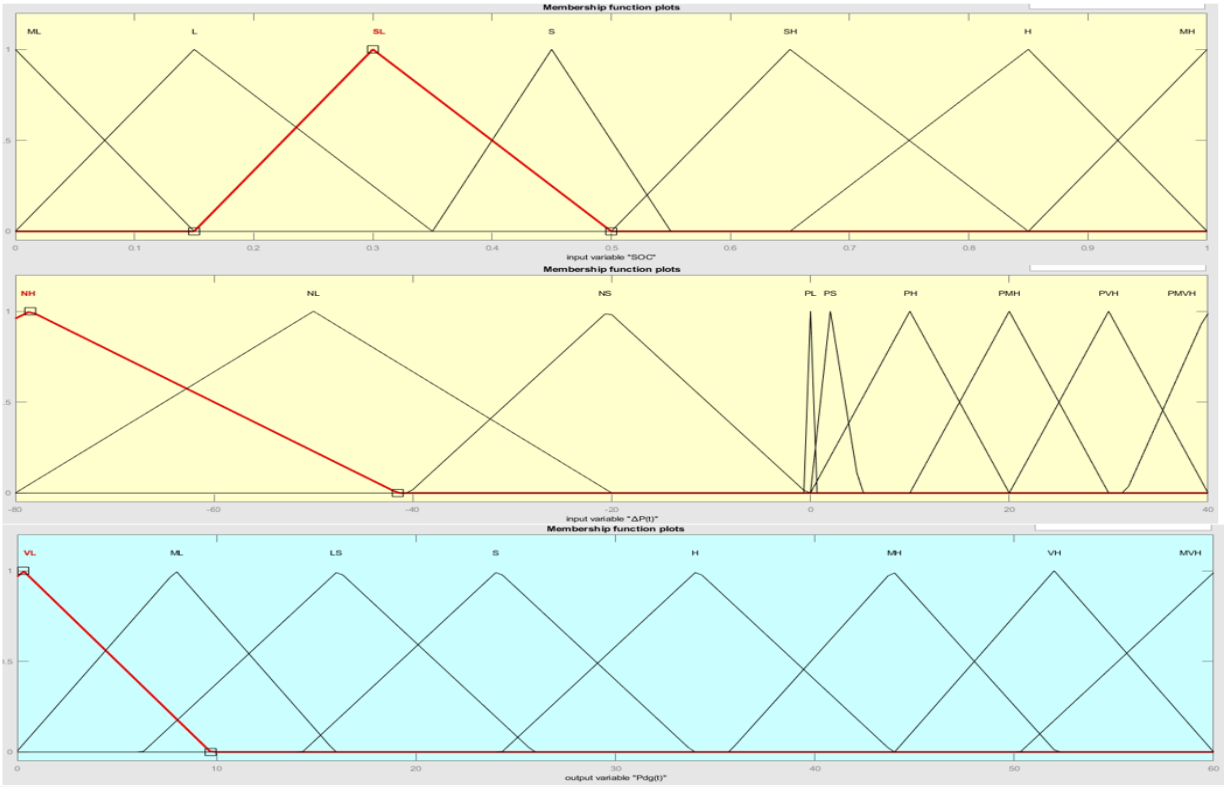


Figure 3.6: The membership functions of the FLC2 variables

## 3.2 Formation of FLC1 Rules

The fuzzy logic rules for FLC1 are shown in Table 3.1. The power difference (ΔP) between the current power demand and the current renewable power is the first input into FLC1, while the battery state of charge (SOC) is the second input. The controller uses the value of ΔP and SOC at each time to determine whether to charge the battery or discharge the battery. The correction power factor, $C_{batt}$ is the output of FLC1 that determines how much energy is used to charge the battery or is discharged from the battery. Figure 3.7 shows the three-dimensional view of the output of the FLC1 controller.

Table 3.1: Fuzzy-Logic Rule Table for FLC1

| ΔP(t)/SOC | Multiplier ($C_{batt}$) | | | | | | |
|---|---|---|---|---|---|---|---|
| | ML | L | SL | S | SH | H | MH |
| NH | MH | MH | MH | MH | MH | MH | ML |
| NS | MH | MH | MH | MH | MH | MH | ML |
| NL | MH | MH | MH | MH | MH | MH | ML |
| PL | ML | ML | ML | ML | MH | MH | MH |
| PS | ML | ML | ML | ML | MH | MH | MH |
| PH | ML | ML | ML | ML | MH | MH | MH |

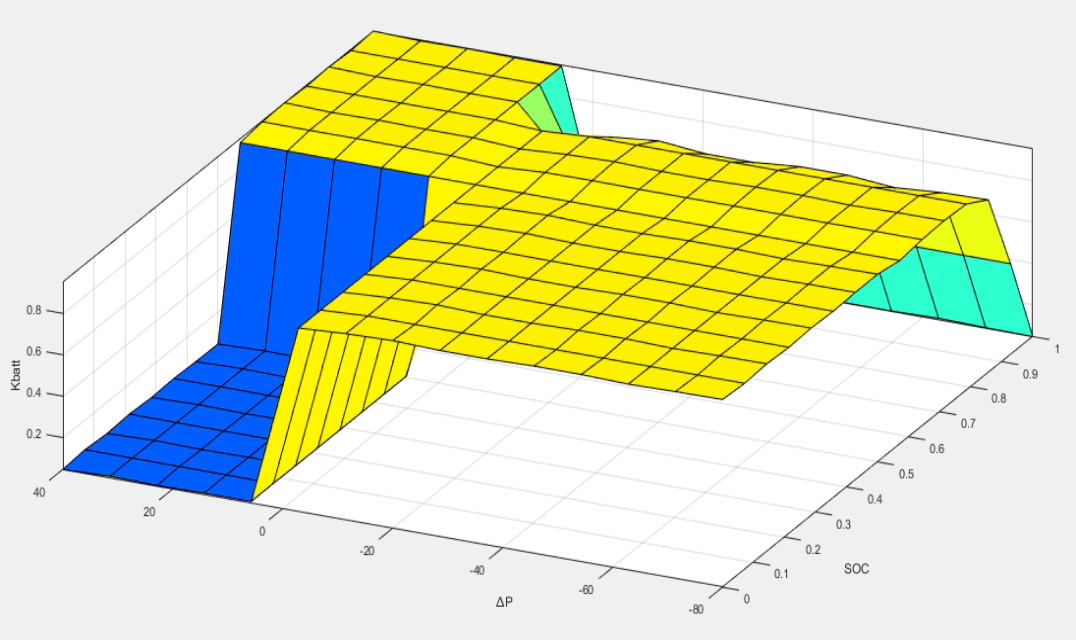


Figure 3.7: Three-Dimensional plot of FLC1 Rules

### 3.3 Formation of FLC2 Rules

Fuzzy logic rules for FLC2 are shown in Table 3.2. FLC2 decides when to switch on the diesel generator to power the excess load. The power gap (ΔP'), which is the net load minus the battery discharging power and the previous state of charge (SOC(t-1)), are the inputs to FLC2. The controller uses values of (ΔP') and SOC(t-1) to decide whether to start the DG or not. When the SOC is low and there is excess load, the controller starts the DG. When the SOC is low, and there

is excess RE, the controller will not start the DG. When the SOC is high and there is excess load, the controller will not start the DG. The controller will start the DG when there is excess RE and SOC is high. The DG power ($P_{DG}$), the FLC2 output, supplies the load, and the extra energy from the DG is used to charge the battery. Figure 3.8 shows the three-dimensional view of the output of the FLC2 controller.

Table 3.2: Fuzzy-Logic Rule Table for FLC2

| ΔP(t)'/SOC | $P_{DG}(t)$ | | | | | | |
|---|---|---|---|---|---|---|---|
| | ML | L | SL | S | SH | H | MH |
| NH | VL | VL | VL | VL | VL | VL | VL |
| NL | VL | VL | VL | VL | VL | VL | VL |
| NS | VL | VL | VL | VL | VL | VL | VL |
| PL | VL | VL | VL | VL | VL | VL | VL |
| PS | S | S | S | VL | VL | VL | VL |
| PH | H | H | MH | MH | VL | VL | VL |
| PMH | VH | VH | VH | MH | VL | VL | VL |
| PVH | VH | VH | VH | MH | VL | VL | VL |
| PMVH | VH | VH | VH | MH | VL | VL | VL |

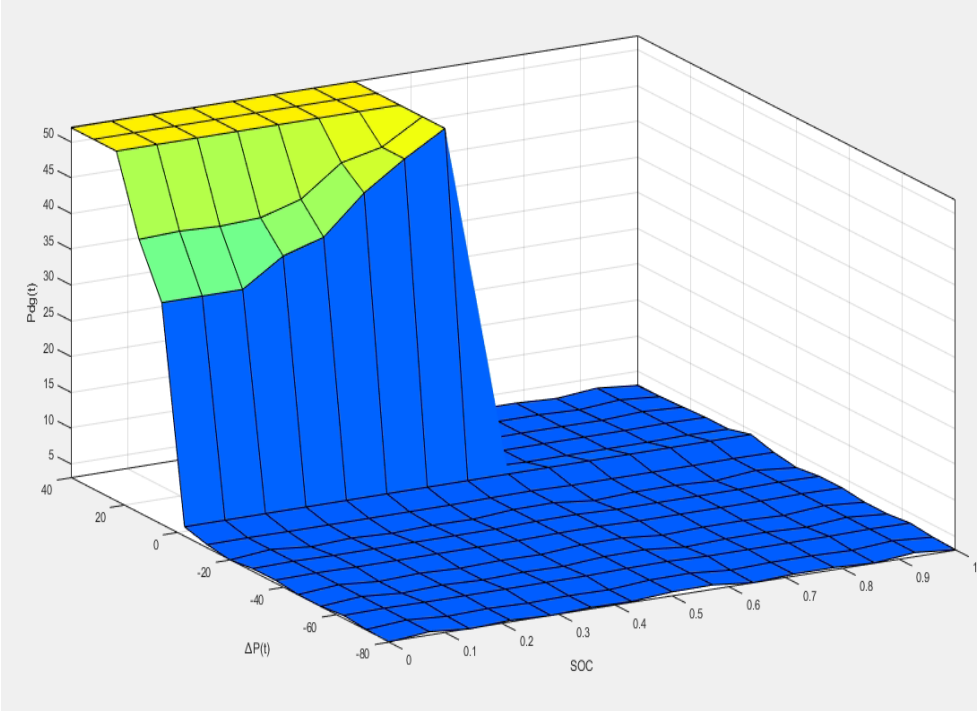


Figure 3.8: Three-Dimensional plot of FLC2 Rules

# Chapter 4

# Data and Case Study

This study arose from the desire to investigate and understand the cost of providing affordable and reliable electricity for off-grid communities and to present the potential cost implications and benefits of off-grid electrification projects as guides for developers, investors, and policymakers and to consequently increase the renewable energy electrification of off-grid communities. To achieve this, real data were used to reduce assumptions to the minimum possible. Several visits to the case study community were made to understand the load demand, consumers' behaviors, weather conditions, number of households, and other factors that affect the electricity consumption in the community. Several visits were also made to the solar mini-grid site operating in the community to acquire information about the load demand and the overall financial requirement of generating and distributing electricity in the off-grid rural community.

## 4.1 Case Study

The case study is an isolated off-grid rural community called Olooji in the Ijebu-East Local Government Area of Ogun state, Nigeria. Olooji is an agrarian community located on latitude $N06^0$ 53.329' and longitude $E04^0$ 27.342'. Olooji falls within the tropical rain forest, which is typical of the regions in the southern part of Nigeria. It has two seasons, the dry season (October-March) and the wet season (April-September). The number of households in Olooji is about six hundred (600), with an average size of 11 people per household, comprising majorly of children and women. Olooji is estimated to have a population of up to 7,000 people. The community is about sixty (60) kilometers and around two hours drive on an untarred muddy road from the nearest National Grid at *Orita J4 Express* community. Olooji heads over ten (10) nearby villages and runs on a self-employed agrarian economy with mainly female merchants displaying agricultural produce, food, and clothing in roadside shops. Merchants from Lagos, Ijebu-ode, Ore, and bigger towns and cities come daily to buy goods in Olooji. Their farm crops are majorly Cocoa, Palm Oil, Timber, Plantain, and Kola Nut. Commercial and creative enterprises such as barbing, tailoring, welding, provision store, viewing centers, bar, restaurants, oil milling, and pepper milling are numerous in the community. Olooji is currently being electrified by a solar mini-grid system constructed and operated by ACOB Lighting Technology Limited, a private solar mini-grid developer in Nigeria. Figure 4.1 shows the satellite view of the Olooji community (courtesy of Google Earth), while Figure 4.2 shows the aerial view of the Olooji community.


Figure 4.1: Satellite view of the Olooji community (courtesy of Google Earth)

Figure 4.2: Aerial view of the Olooji community

### 4.1.1 Load Profile

The hourly load demand of the Olooji community for 24 hours was collected from the daily records by the mini-grid operator via their SMA platform. Figure 4.3 below shows the typical daily load profile of the Olooji community as obtained from the developer's load monitoring platform. From the daily load profile, the hourly average consumption in the community was 23.3kWh and the annual energy consumption in the community was estimated to be 202MWh.

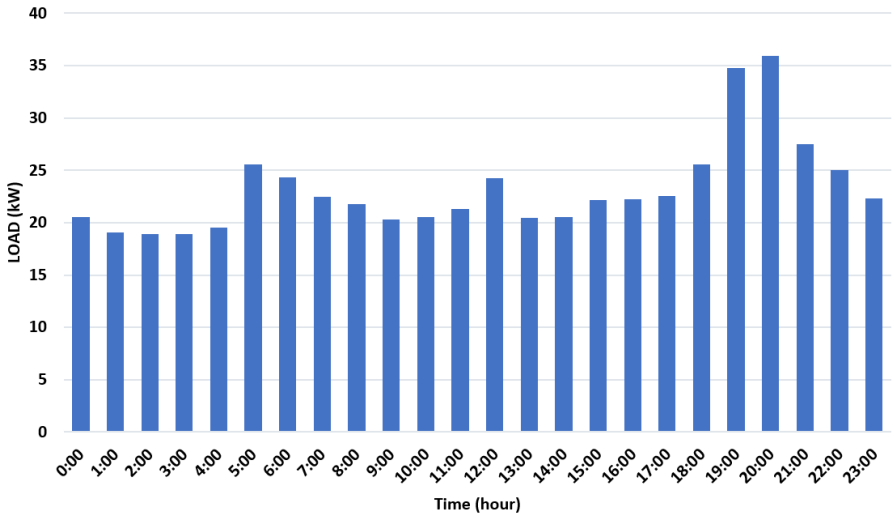


Figure 4.3: Typical daily load profile of Olooji community

### 4.1.2 Solar Irradiance, wind speed and temperature data

Olooji solar irradiation, wind speed and temperature data for one year running from January 1st, 2016, to December 31st, 2016 (Figure 4.4-4.6), was collected from the National Aeronautic Space Agency (NASA) website.

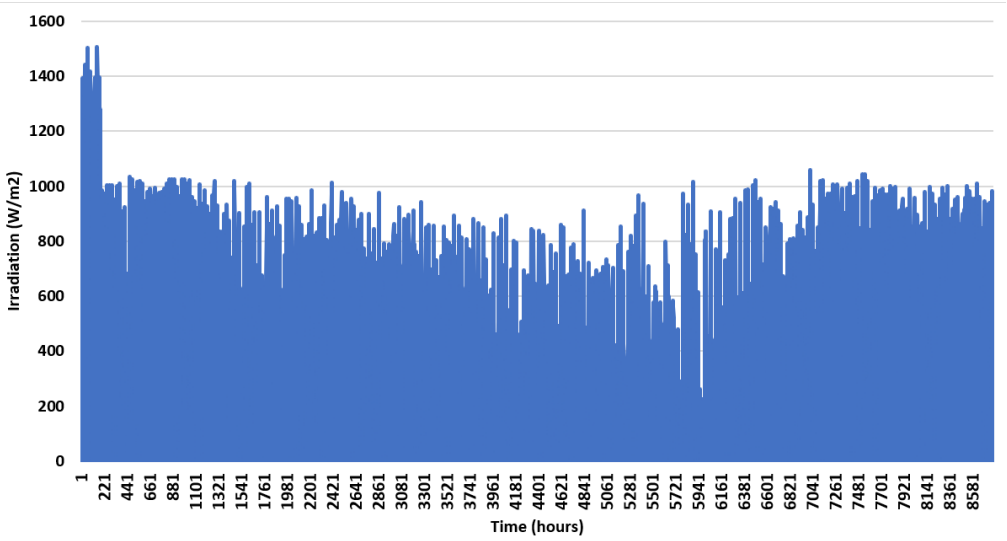


Figure 4.4: Olooji Irradiation Data for one year

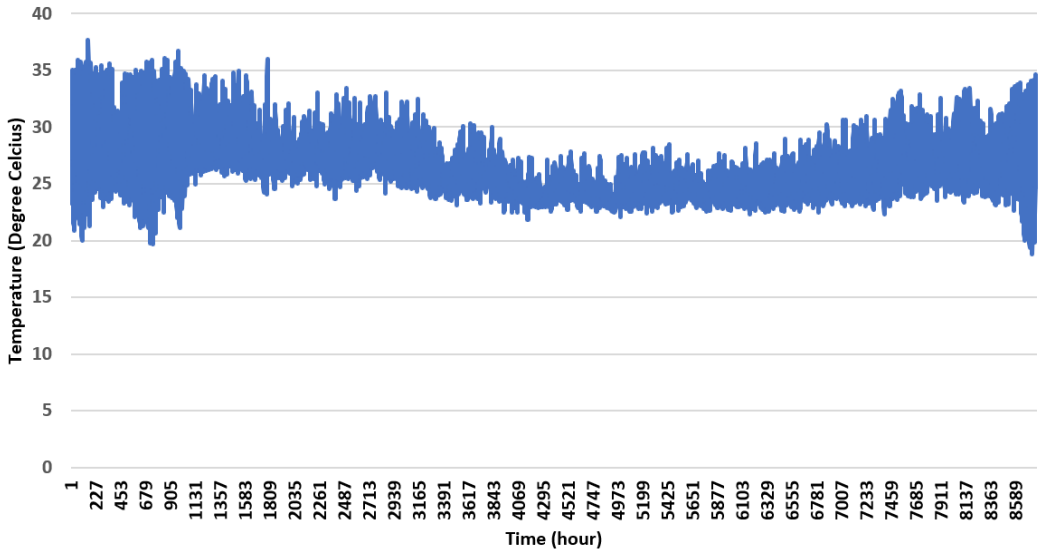


Figure 4.5: Olooji Temperature Data for One year

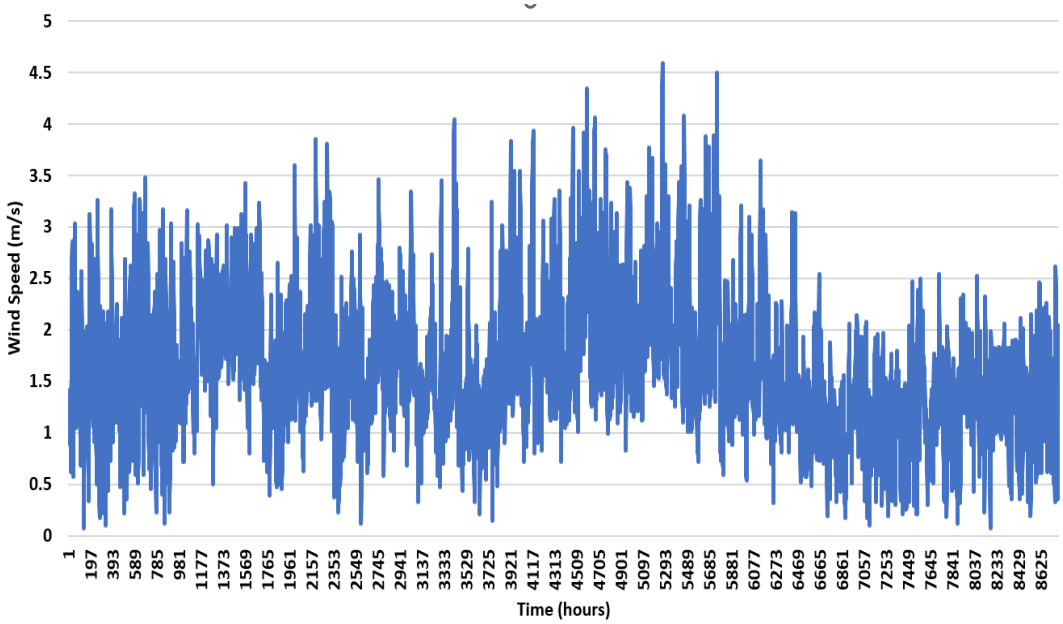


Figure 4.6: Olooji Wind Speed Data for One year

### 4.2 Battery lifecycle

The battery lifecycle was determined using the graph that shows the service life in cycles versus the Depth of Discharge (DOD) in the datasheet from Hoppecke battery Original Equipment Manufacturer (OEM), shown in Figure 4.7 [43]. Figure 4.8 represents the cost of operation plotted under different State of Charge (SOC) ranges [22], the best operating cost, when DG is used in HRES, is at the lower bound SOC of 55% and the upper bound SOC of 75%. For this research, the lower bound SOC considered is 55% which corresponds to a DOD of 45%, and the upper

bound SOC considered is 80% which corresponds to a DOD of 20%. The battery was assumed to run a daily cycle. This means that the battery is being charged to the maximum SOC and fully discharged to the minimum SOC daily (every 24 hours).

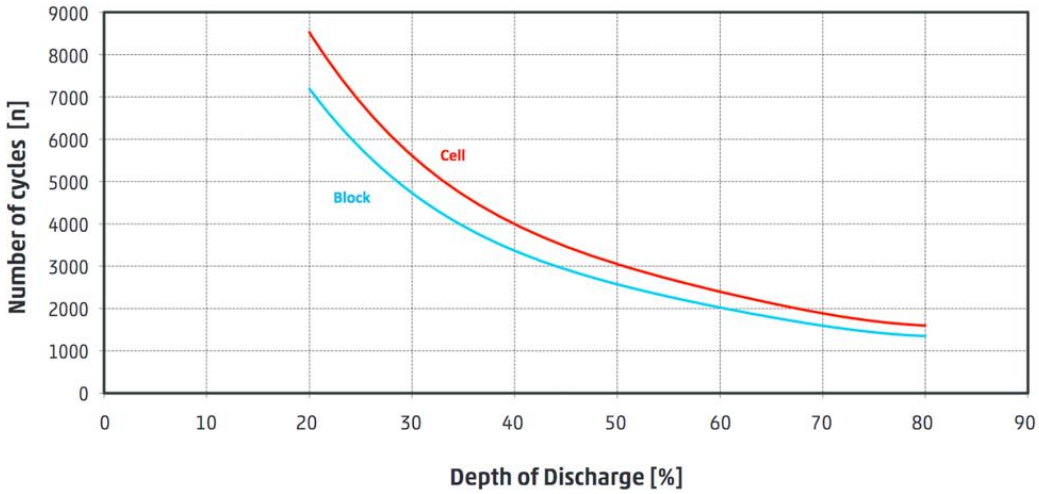


Figure 4.7: Number of cycles versus Depth of Discharge (adopted from [43] )

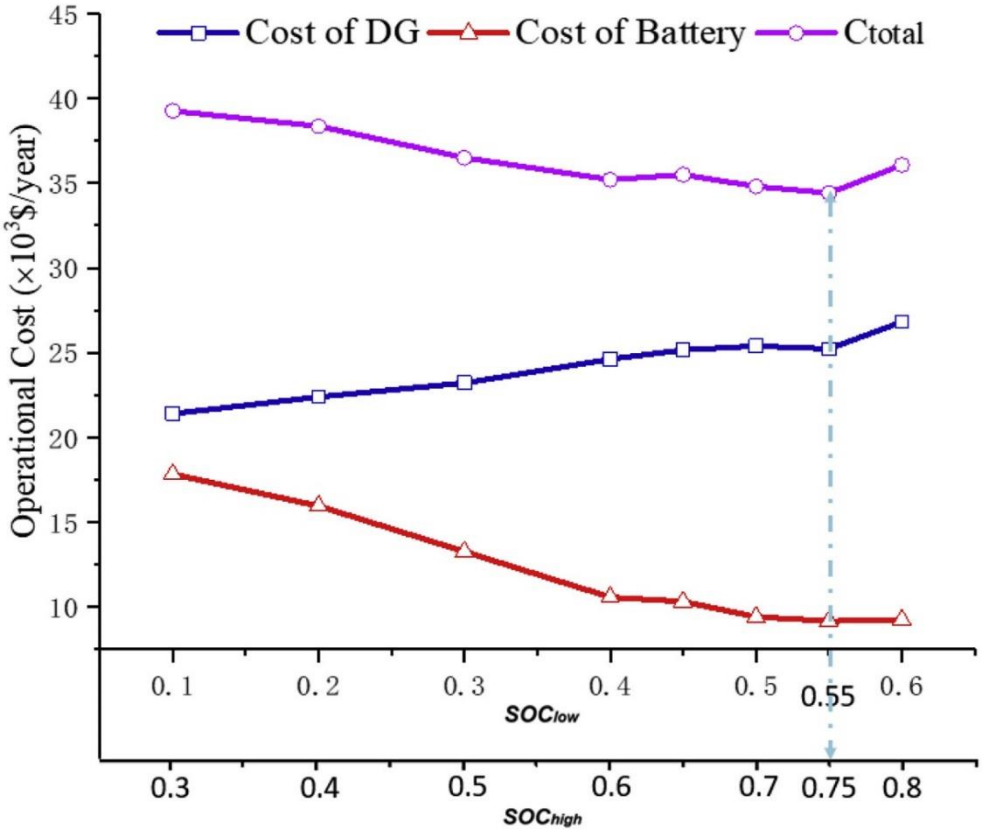


Figure 4.8: Cost of operation under different SOC ranges (adopted from [22])

### 4.3 Investment Cost analysis

The investment costs of the HRES components are given in Table 4.1. The values were derived primarily from the financial budget for implementing a solar mini-grid site from ACOB Lighting Technology Limited, the mini-grid operator. The costs of the equipment were collected from the Original Equipment Manufacturers (OEMs) and surfing the OEM websites. The initial costs are considered as follows:

- PV panels and accessories, including the PV cable and mounting accessories.
- Battery and battery accessories, including battery cable and battery rack.
- Diesel generator (DG) and DG accessories.
- Inverter and inverter accessories
- Distribution costs, including the cost of erecting electric poles, Aluminum Conductor Steel Reinforced (ACSR) cable, recline cable, and stay wires.
- Metering includes the meter, protective circuit breaker (PCB), and Data Concentrator Unit (DCU) to monitor consumers' consumption.
- Development and installation costs, including the cost of the land acquisition, cost of land clearing and preparation, cost of feasibility studies, Environmental Impact Assessment (EIA) cost, technical design cost, Nigerian Electricity Management Service Agency (NEMSA) permit cost, Nigeria Electricity Regulatory Commission (NERC) license cost, Rural Electrification Agency (REA) license cost, and cost of acquiring the land title/ Certificate of Occupancy (C of O) by the state government.
- Wind turbines and accessories costs collected from ATO, a manufacturer of wind turbines.
- Fuel cost was estimated at 1.57 USD/liter, the equivalent of 700 NGN/liter, the prevailing diesel price in Nigeria as of June 2022. The interest rate of 11.5% was Nigeria's prevailing interest rate as of June 2022.

Table 4.1:Investment Cost Analysis

| **Equipment** | **Initial cost ($/kW)** | **Lifetime(years)** | **Efficiency** |
|---|---|---|---|
| PV (includes PV cable, PV mounting accessories) | 704.63 | 24 | |
| Wind Turbine and Wind Turbine installation accessories | 1619.74 | 24 | |
| Battery (includes battery cable and battery rack) | 188.17 | 16 | 0.85 |
| Diesel generator (DG accessories, ATS,) | 156.13 | 24,000 hours | |
| Inverter and accessories | 645.69 | 24 | 0.92 |
| PV controller (includes accessories) | 102.09 | 24 | 0.95 |
| Wind Turbine Controller and accessories | 102.09 | 24 | 0.95 |
| Construction (Powerhouse, Fencing, PV array Foundation) | 357.32 | | |
| Development and Installation | 320.33 | | |
| Distribution and Metering | 1063.70 | | |
| Fuel costs | 1.57 $ per liter | | |
| Interest rates | 11.5 | | |
| Project Lifetime | | 24 | |
| Operation and Maintenance Cost | 20% of the Initial cost | | |

### 4.4 Wind turbine characteristics

The wind turbine parameters used are shown in Table 4.2. The wind turbine characteristics were obtained from the datasheet of a 1000W wind turbine made by ATO. The datasheet is shown in Figure 4.9.

Table 4.2: Wind Turbine Parameters

| | |
|---|---|
| Blade diameter | 2.4m |
| Blade radius | 1.2m |
| Start-up wind speed | 2.5m/s |
| Rated wind speed | 12.5m/s |
| Cut-out (survival) wind speed | 40m/s |
| Rated power | 1kW |
| Maximum Output Power | 1.05kW |

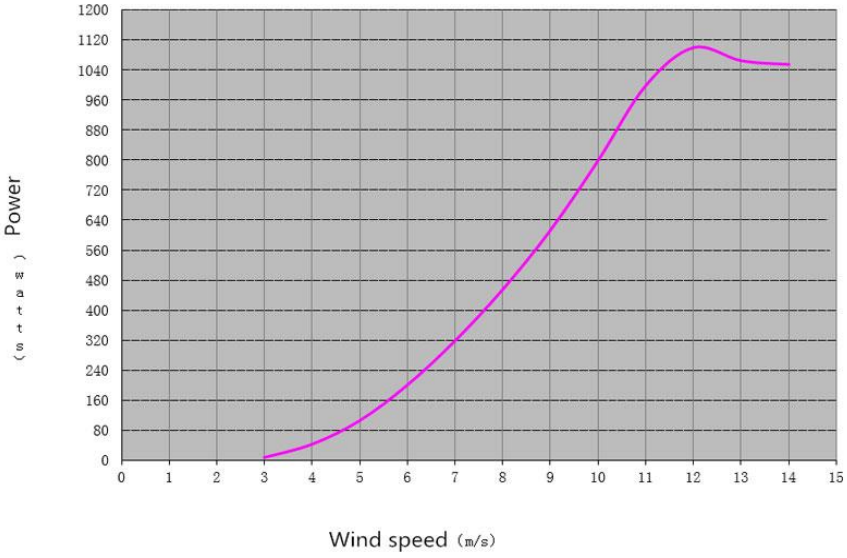


Figure 4.9:1000W wind turbine characteristics (by ATO)

# Chapter 5

# Results and Discussion

## 5.1 Size optimization results

The boundary values used are shown in table 5.1. Table 5.2 shows the result of the developed PSO codes that were run for 100 iterations for the two scenarios.

Table 5.1: Basic assumptions used in two scenarios.

| Equipment | 1st Scenario | | 2nd Scenario | |
|---|---|---|---|---|
| | Minimum capacity | Maximum capacity | Minimum capacity | Maximum capacity |
| PV | 0 kW | 150kW | 0kW | 100kW |
| Wind Turbine | 0 kW | 100kW | 0kW | 100kW |
| Battery | 0kWh | 2000kWh | 0kWh | 700kWh |
| Generator | 0 kW | 100kW | 0kW | 100kW |

Table 5.2: Result of the PSO optimization algorithm

| Equipment Capacity | 1st Scenario | 2nd Scenario |
|---|---|---|
| PV | 130 kW | 100kW |
| Wind Turbine | 0 kW | 0kW |
| Battery | 1370 kWh | 700kWh |
| Generator | 0 kW | 25kW |
| LPSP | 0.20% | 0.05% |
| LCOE | 0.48 USD/kWh | 1.17 USD/kWh |

The LCOE for scenarios 1 and 2 was estimated at 0.48 USD/kWh (@ LPSP= 0.20%) and 1.17 USD/kWh (@ LPSP= 0.05%), respectively. For the two scenarios, wind power was not used. This could be explained because the wind speed in the case study community is deficient. Hence, using the wind turbine to meet the extra energy required would be more expensive. The second scenario required a diesel generator that was not needed in the first scenario. this raised the LCOE higher by more than 150% due to the excessive cost of fuel required to run the diesel generator. In both

scenarios, the LPSP of 0.2% and 0.05% were within acceptable limits, ensuring adequate and reliable electricity supply to the community.

The effect of the two seasons (dry and wet seasons) in Nigeria can be compared from the combined graphs of the simulation output. Figure 5.1 shows the power distribution of all energy sources using one (1) week of data in January (dry season) in the first scenario, while Figure 5.2 shows the power distribution of all energy sources using one (1) week of data in August (wet season) in the first scenario. Figure 5.3 shows the distribution of all energy sources using one (1) week of data in January (dry season) in the second scenario, while Figure 5.4 shows the distribution of all energy sources using one (1) week of data in August (wet season) in the second scenario. Figures 5.5 and 5.6 show the battery SOC for one week in August and January, respectively. Figures 5.7 and 5.8 show the LCOE for the first and second scenarios respectively.

It can be seen from the power distribution of each month that the solar power generation during the wet season (August) was low compared to that of the dry season (January). However, in the first scenario, a diesel generator was not used for both the dry and the rainy seasons. In the second scenario, the diesel generator was used for the two seasons and more hours during the wet season in August than during the dry season in January. The diesel generator was used during most of the nights in August to compensate for the deficiency in the renewable energy generated.

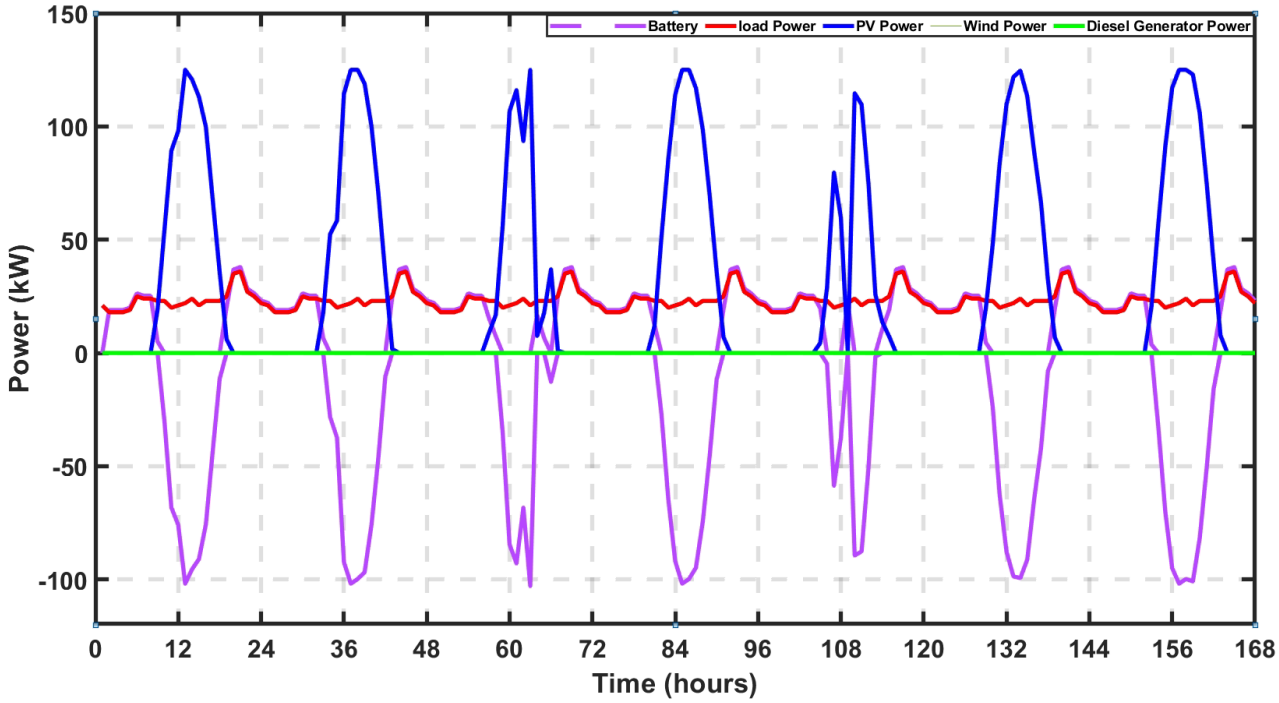


Figure 5.1: Power distribution of all energy sources in the first scenario January

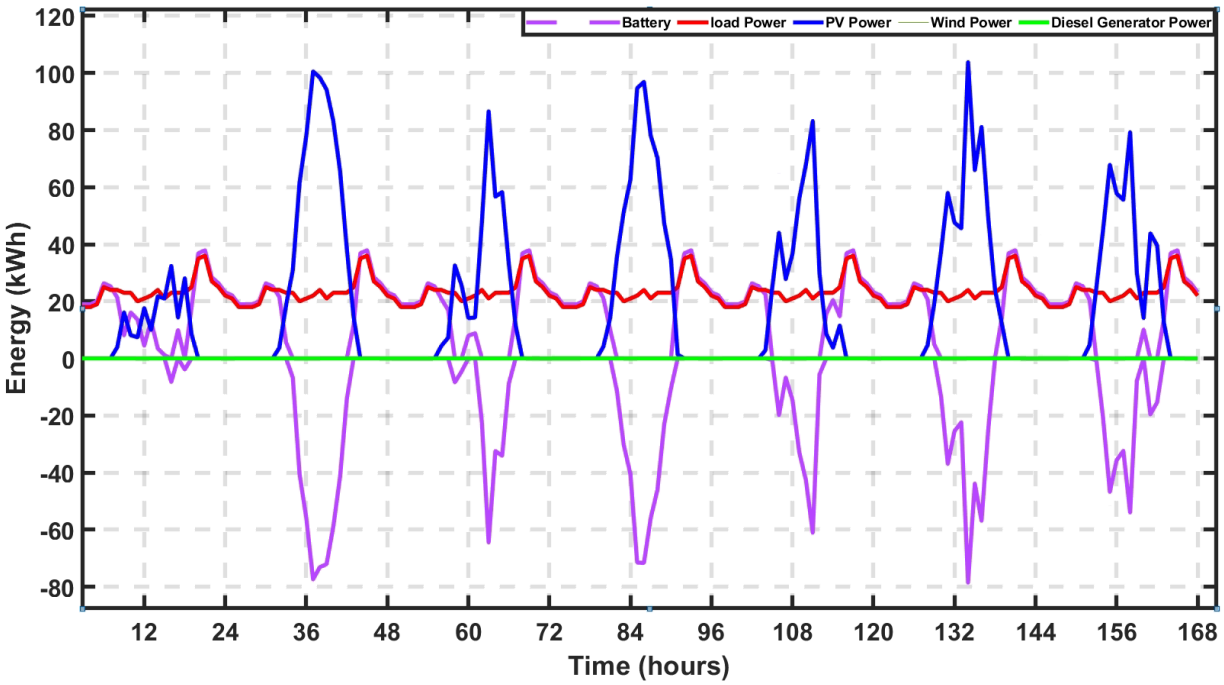


Figure 5.2: Power distribution of all energy sources in the first scenario (August)

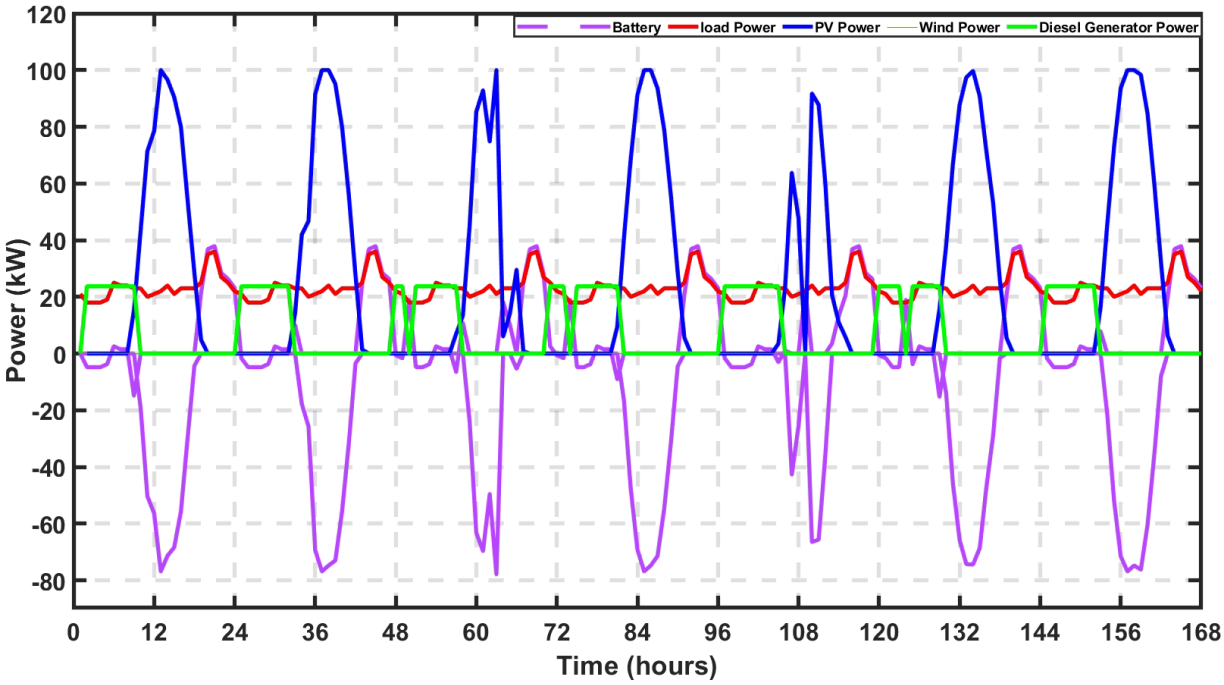


Figure 5.3: Power distribution of all energy sources in the second scenario January

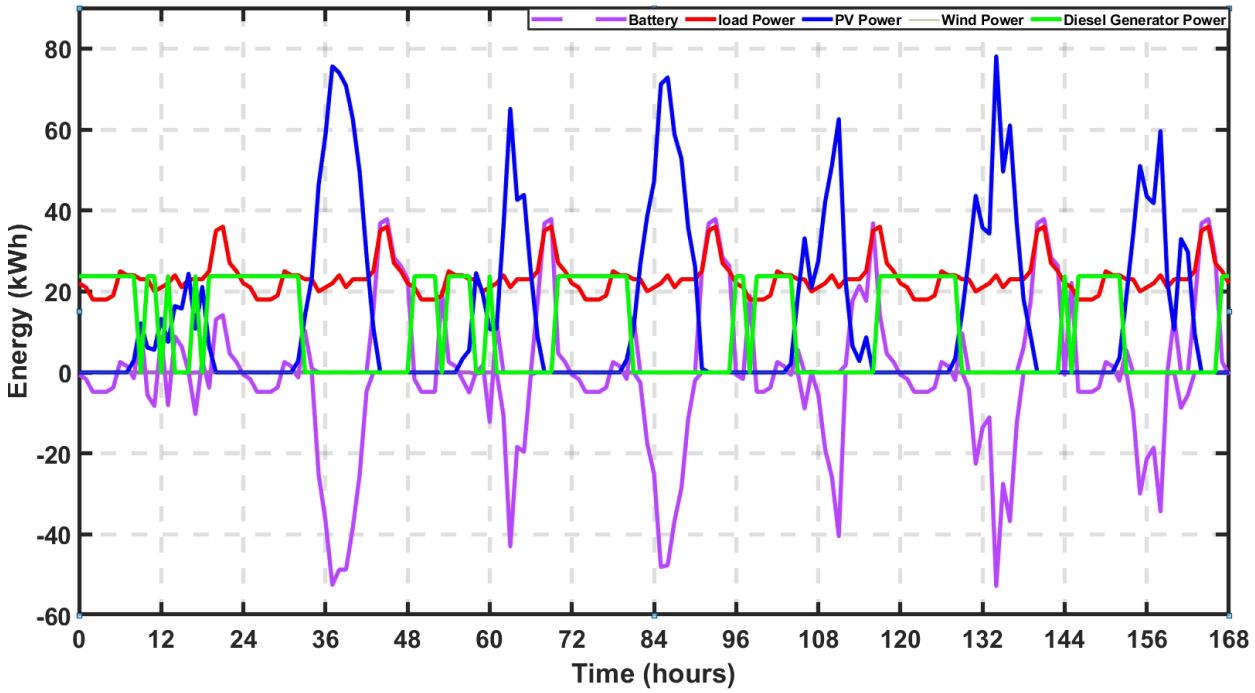


Figure 5.4: Power distribution of all energy sources in the second scenario (August)

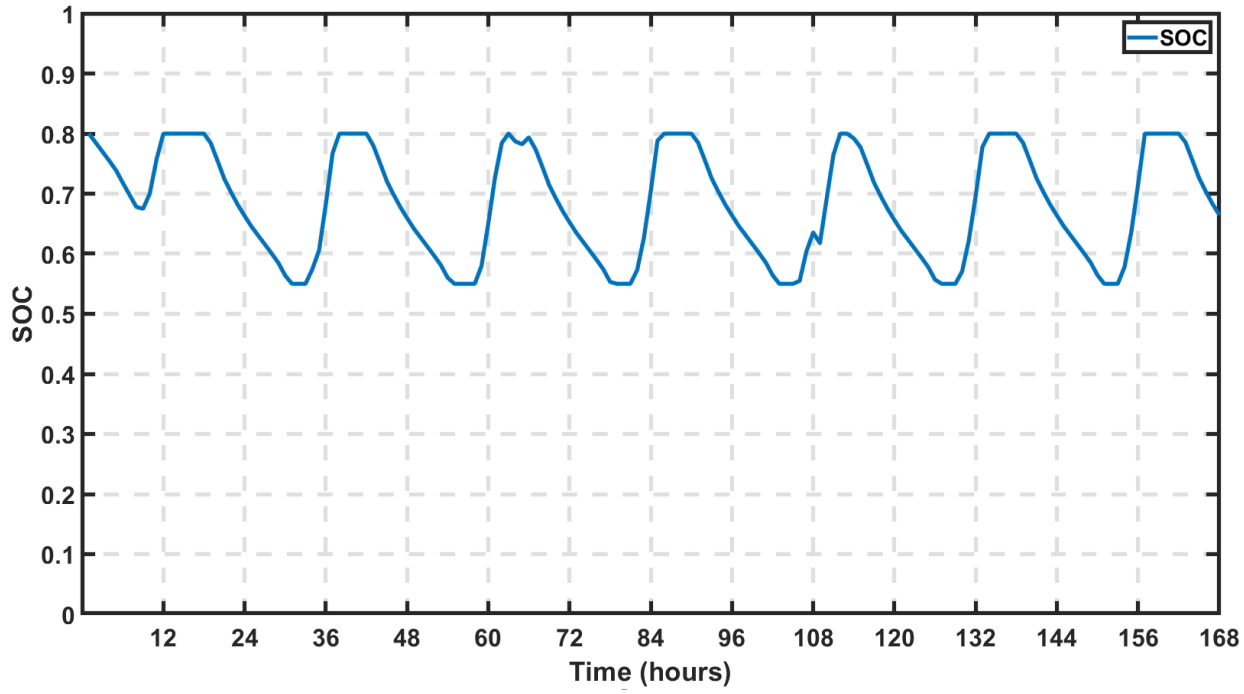


Figure 5.5: SOC for week in January

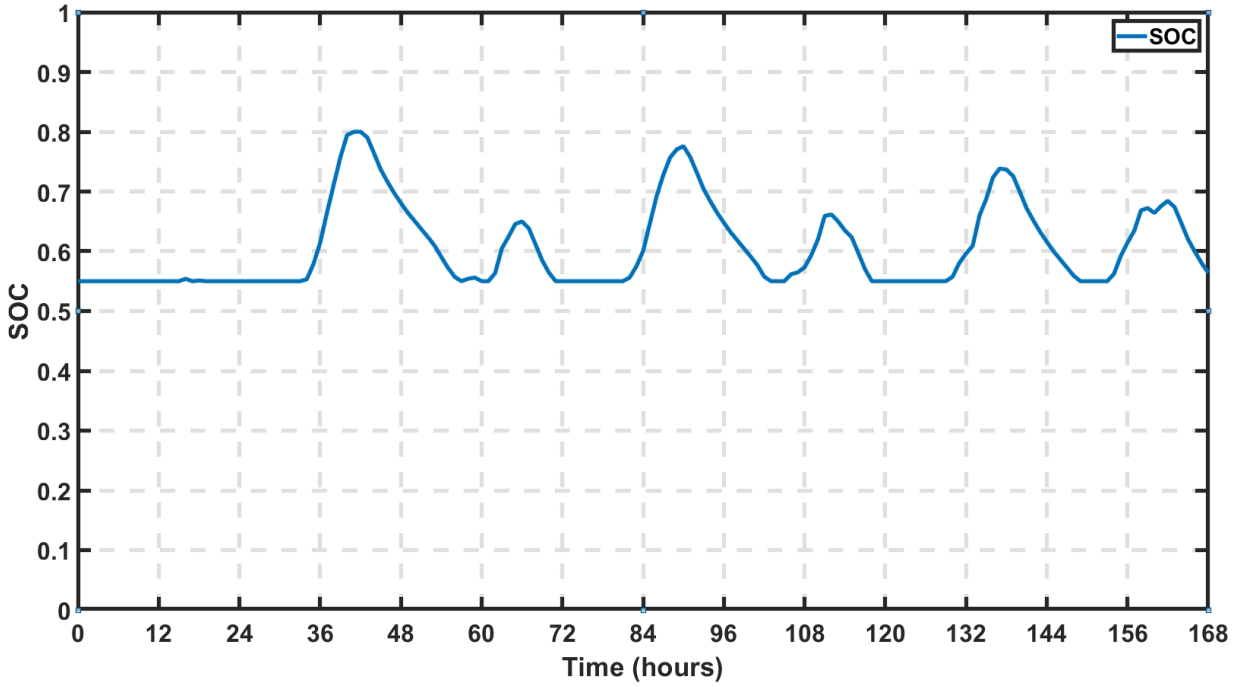


Figure 5.6: SOC for one week in August

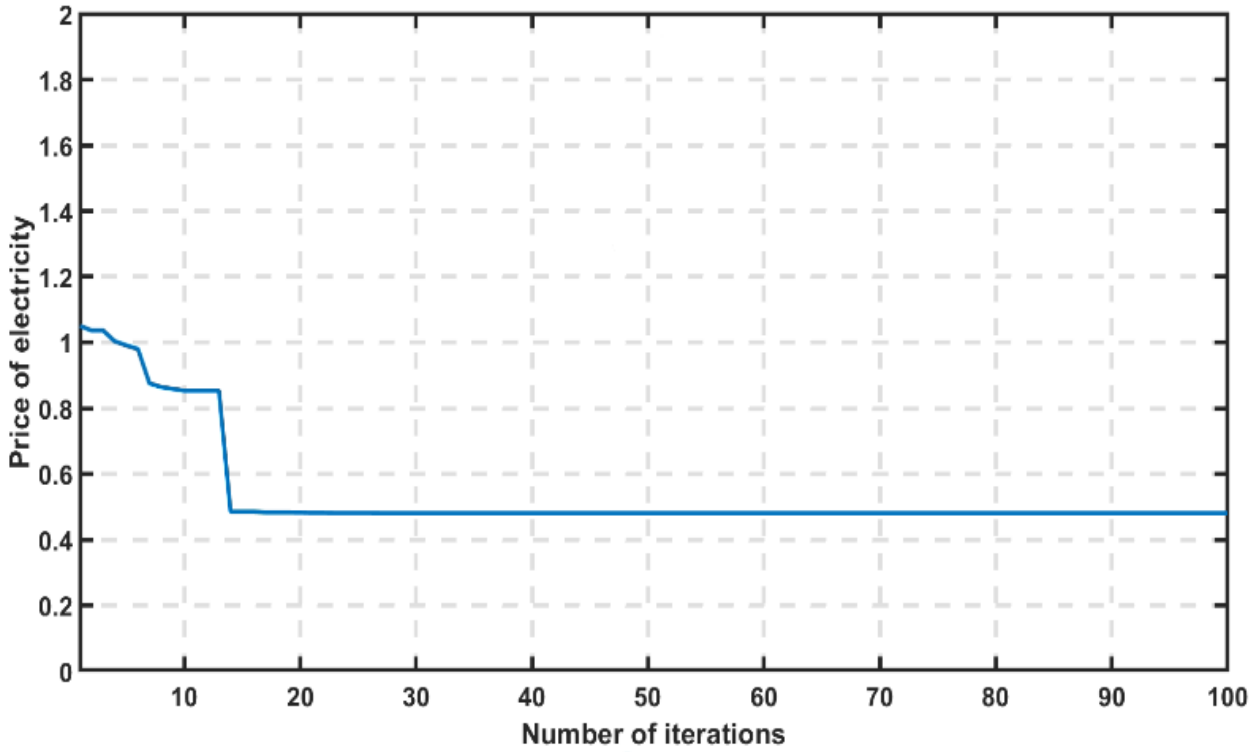


Figure 5.7: LCOE for 100 iterations-First Scenario

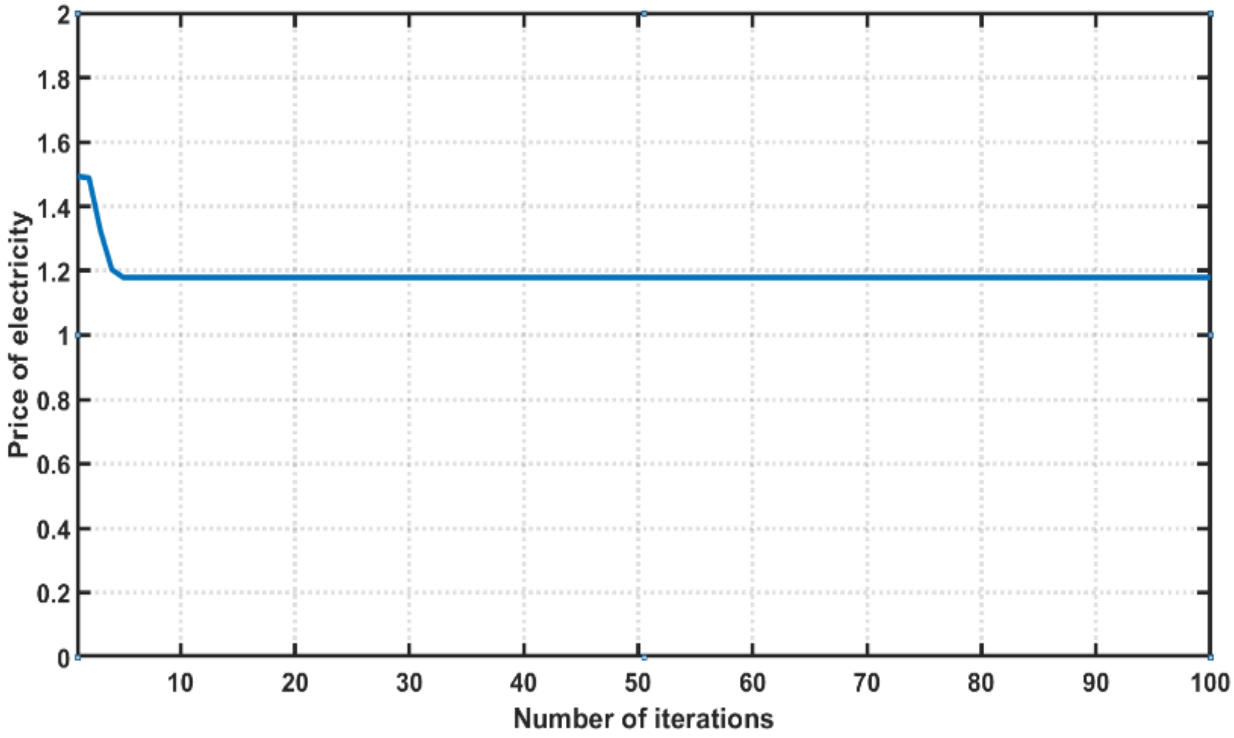


Figure 5.8: LCOE for 100 iterations-Second Scenario

## 5.2 Annual Energy Contributed by Each Energy Source

Table 5.3 shows the annual energy contributed by each energy source for scenarios 1 and 2. The percentage contributed by each source is shown in the pie charts below. Figure 5.9 is the pie chart of the percentage contributed for scenario 1, and Figure 5.10 is the pie chart of the percentage contributed for scenario 2. The monthly energy contributed by each energy source for the first scenario is shown in Figure 5.11; solar energy is the only energy source available for scenario 1 while the monthly energy contributed by each energy source for the second scenario is shown in Figure 5.12. For both scenarios, the seasonal effects can be seen in the amount of energy generated from the PV. More solar energy was produced during the dry season (October-March), and lesser diesel energy was used. On the other hand, lesser solar energy was produced during the rainy season (April-September), and more diesel energy was used. For both scenarios, the total annual energy generated equaled the total annual energy demanded plus the total annual lost energy factored into the efficiency of the equipment.

Table 5.3: Annual Energy Contributed by Each Energy Source

| | Scenario 1 (MWh) | Contribution | Scenario 2 (MWh) | Contribution |
|---|---|---|---|---|
| PV Energy | 226.76 | 100% | 151.14 | 65% |
| Wind Energy | 0 | 0% | 0 | 0% |
| Diesel Generator | 0 | 0% | 81.2 | 35% |

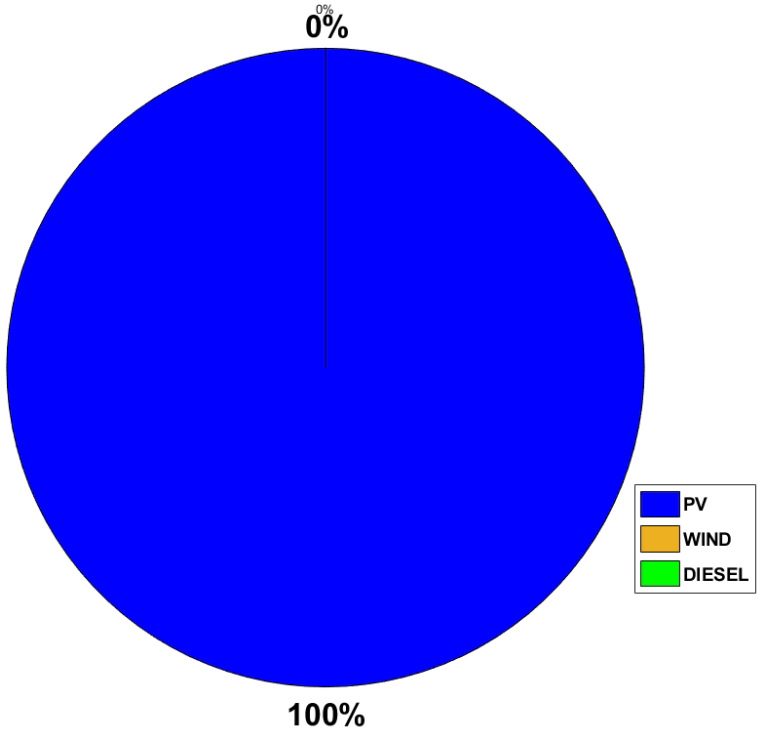


Figure 5.7: Percentage Annual energy contribution by each source (First Scenario)

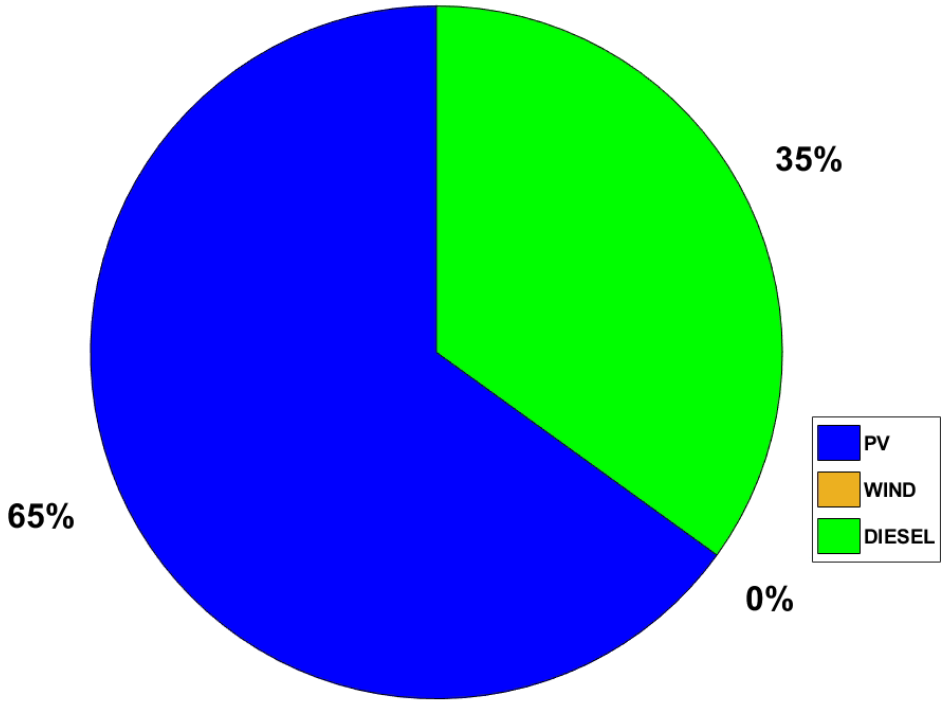


Figure 5.8: Percentage Annual Energy Contribution by Each Source (Second Scenario)

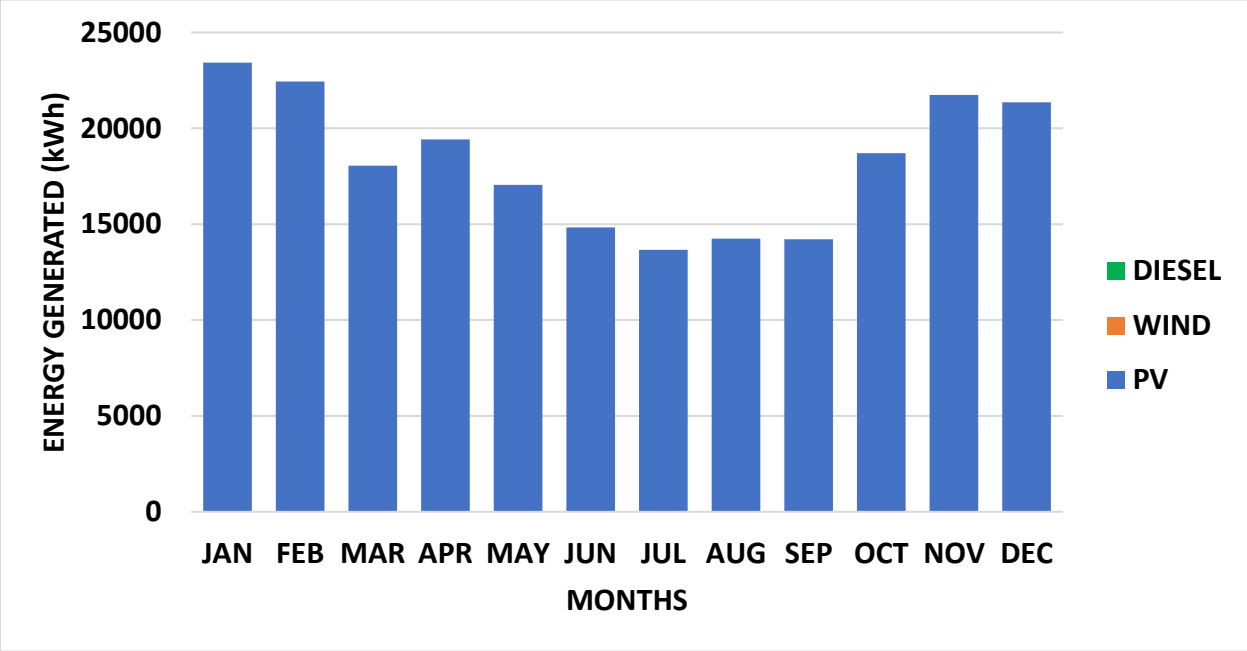


Figure 5.11: Monthly Energy Contribution by Each Source (First Scenario)

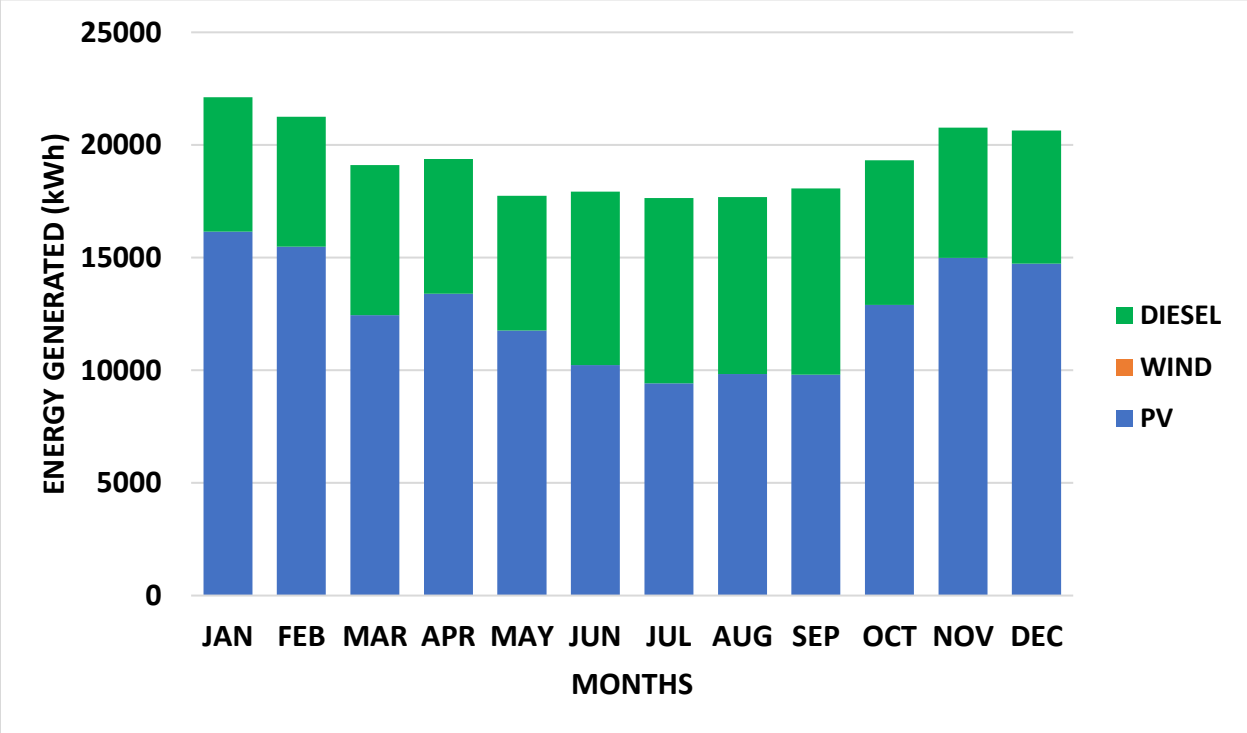


Figure 5.12: Monthly Energy Contribution by Each Source (Second Scenario)

### 5.3 Comparing the LCOE result with LCOE from other studies

The LCOE result from this study was compared with LCOE results from other studies on HRES as shown in Table 5.4. The system configuration of the compared studies includes solar PV, wind turbine, battery, and diesel generator. Cost of equipment, cost of operation, road networks, security, government incentives, and regulation are among the factors responsible for the variation in the LCOE among the different countries.

Table 5.4: Comparing the LCOE from other studies

| System | Country | LCOE($/kWh) | Ref. |
|---|---|---|---|
| This study (PV/Battery) | Nigeria | 0.48 | This study |
| This study (PV/Battery/Diesel) | Nigeria | 1.17 | This study |
| Hybrid wind/ solar PV/ diesel/battery, | India | 0.76 | [35] |
| Solar PV/ wind/diesel | Indonesia | 1.06 | [44] |
| PV/wind/battery/diesel | Japan | 0.88 | [27] |
| Typical off-grid microgrid in Pacific Island: PV/diesel | Pacific Island | 1-1.7 | [27] |
| Solar PV/ diesel/wind/ battery | South Africa | 0.41 | [45] |
| Solar PV/ diesel | Ecuador | 0.46 | [46] |

### 5.4 Fuzzy Logic Controller results

The performance indicators for the fuzzy logic-controlled EMS are the SOC of the battery and the energy balance of the HRES system. Using the FLC-EMS, the SOC is expected to be kept within a certain range to ensure battery longevity. The energy balance of the HRES system for each time unit measures the effectiveness of the EMS. The energy balance is the summation of all energy sources minus the load and is expected to be zero if the supply meets the demand at each time. Figures 5.13 and 5.14 are the combined diagram of all energy sources for January and August, respectively. These figures show that the energy balance (blue line) is equal to zero for each hour, indicating that the Fuzzy Logic controller effectively ensures energy balance.

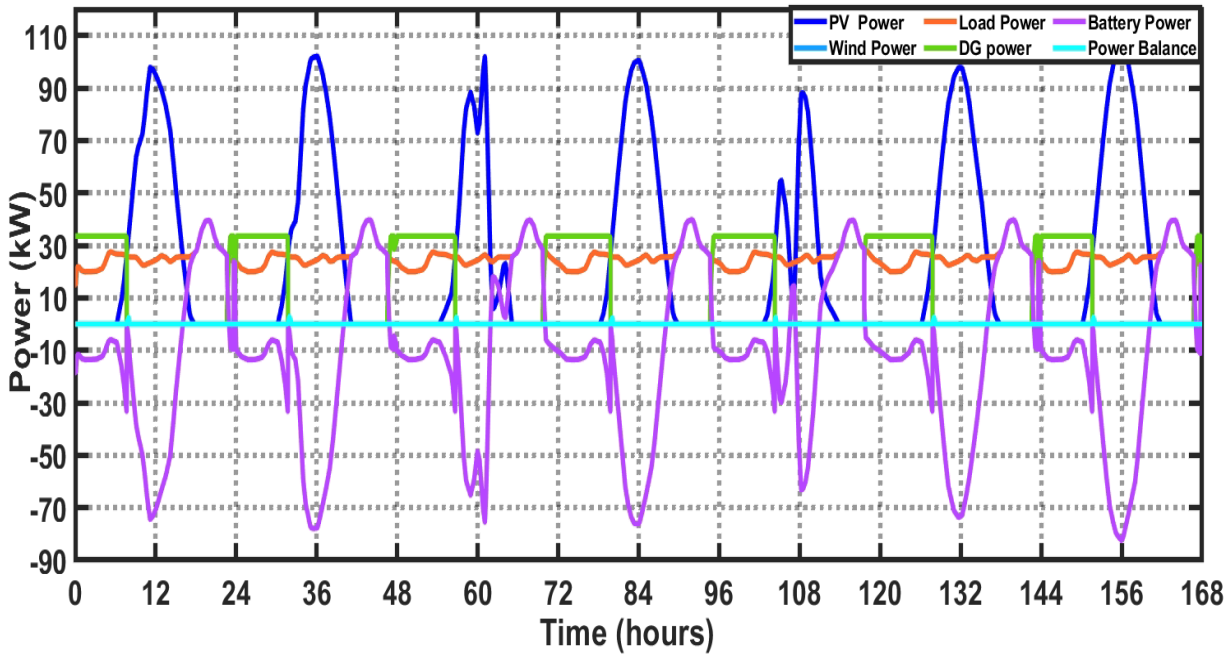


Figure 5.13: Power distribution of all energy sources for One week in second scenario (January)

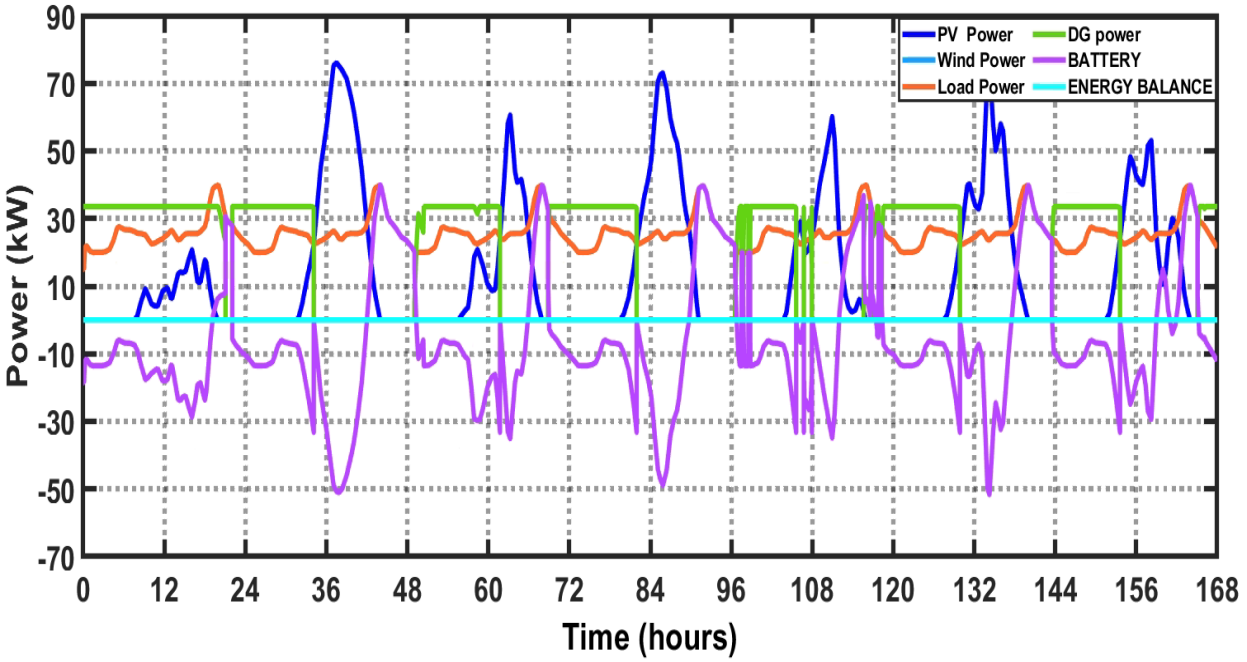


Figure5.94: Power distribution of all energy sources for One week in second scenario (August)

Figure 5.13 shows the combined diagram of all energy sources and the demand for the dry season (January), while figure 5.14 is the combined diagram of all energy sources for the wet season (August). The FLC-EMS enabled the HRES to operate reliably and satisfy the load at each hour of operation. It can be seen that when solar energy was available, it was used to meet the load demand, and excess solar energy was used to charge the battery. When there was no more solar energy, the energy on the battery was discharged to meet the load demand. When the energy on the battery depleted to its minimum state of charge, the diesel generator was switched on to meet the load demand. The diesel generator was switched off immediately; there was energy from the PV the following day.

Furthermore, comparing the two seasons, it can be seen that more solar energy was generated during the dry season than during the wet season, and more DG energy was used during the wet and dry seasons. In either case, there was no output power from the wind turbine as the wind turbine was not considered in this FLC-EMS because the wind turbine sizing from the PSO algorithm was zero. The generator sizing used in the FLC (35kW) was higher than the sizing from the PSO (25kW). This was to provide operating tolerance and stability for the DG. The extra energy from the DG was being used to charge the battery. Also, comparing the graph of the PSO and the FLC, it can be seen that there is a faster response during the energy transition in the case of the FLC than in the case of the PSO. This faster transition offers stability and prevents disruptions during HRES operations. Therefore, FLC-EMS offers stability and optimal utilization of the energy resources during HRES operation; it offers reliable energy irrespective of the weather conditions and load fluctuations. The EMS was able to provide energy to the load both in the dry season and in the rainy season. Figures 5.15 and 5.16 show that the FLC-EMS could keep the battery SOC within the desired range of 55% and 80%.

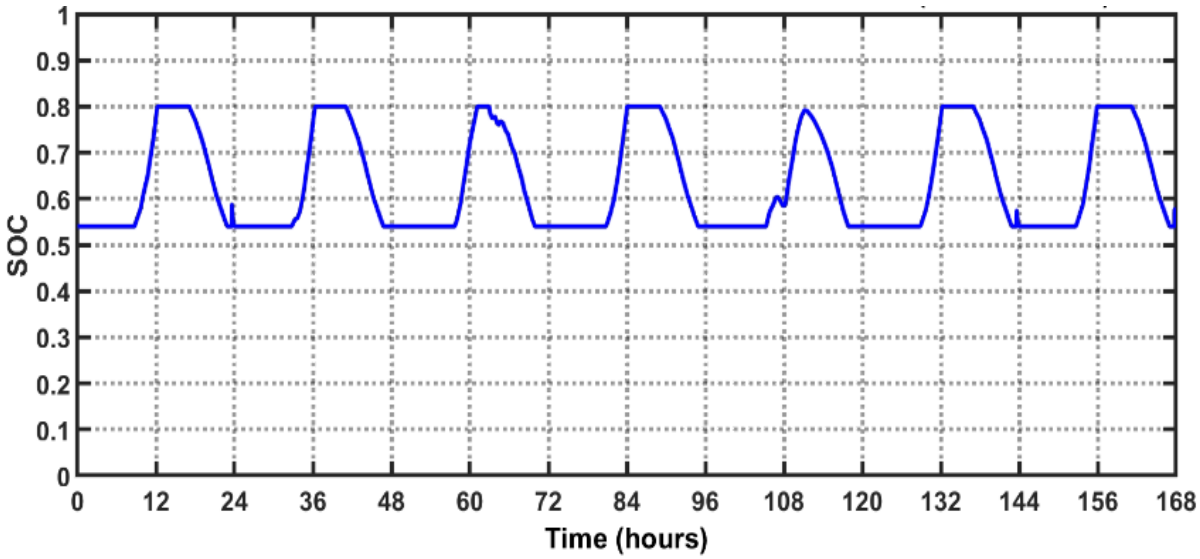


Figure 5.15: State of Charge (SOC) for One week August

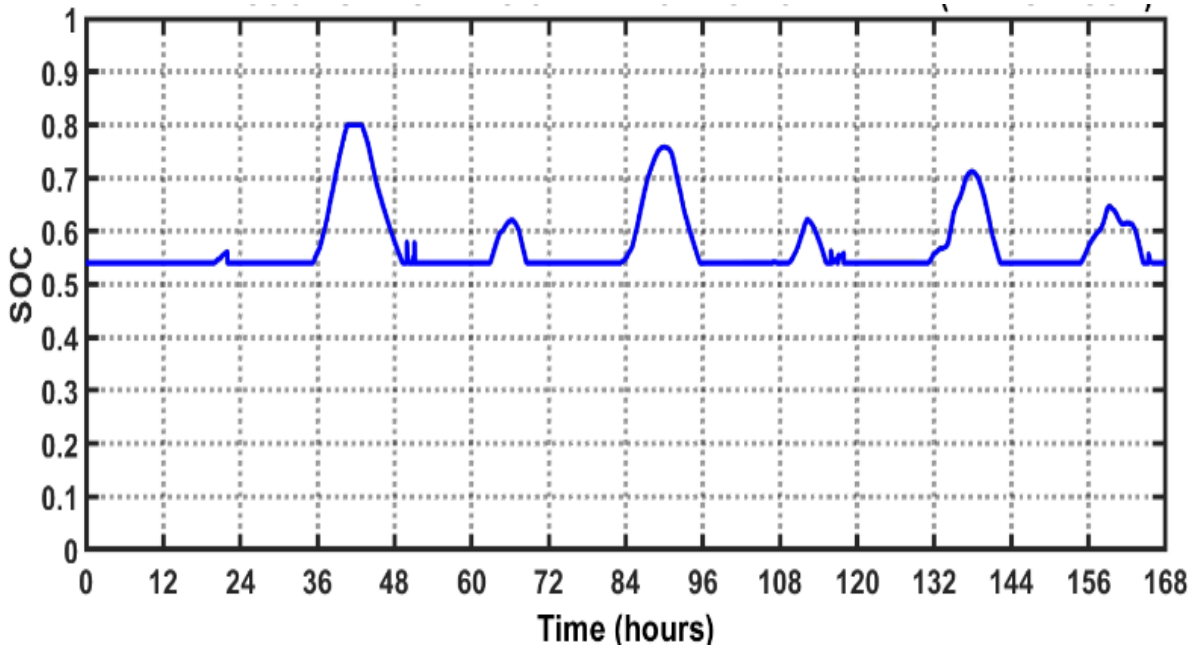


Figure 5.16: State of Charge (SOC) for One week January

# Chapter 6

# CONCLUSION

This research studied the techno-economic analysis of providing a hybrid renewable energy system to an off-grid rural community in Nigeria. The investigated HRES includes the PV, wind turbine, battery, and diesel generator which are used to meet the load demand of an off-grid rural community. The optimal sizing of the HRES equipment was found based on using a least-cost perspective approach which is necessary to ensure the minimum cost of implementation and make the electricity affordable to the consumers. This research also developed a Fuzzy Logic Controlled Energy Management System that ensures an optimal operation and reliability of an HRES system.

Two scenarios were considered for optimal sizing using the proposed HRES. In the first scenario, the LCOE for electrifying the off-grid rural community was found to be 0.48 USD/kWh with the HRES components estimated as: 130kW PV, 0kW wind turbine, 1370kWh battery, and 0kW DG. However, because of the high capital associated with using the maximum battery capacity, a second scenario where half of the maximum capacity would be used was considered. In this scenario, the LCOE for electrifying the off-grid rural community using a hybrid renewable energy system was found to be 1.17 USD/kWh with the HRES components estimated as: 100kW PV, 0kW wind turbine, 700kWh battery, 25kW DG. The results revealed that wind energy could not be considered as an energy source in the two scenarios because of the low wind speed in the region. Furthermore, the effect of the different seasons was observed on the PV power output. More PV power can be generated in the dry season compared to the wet season. Consequently, more renewable energy was utilized to meet the demand in the dry season, and more DG power was used to meet the load demand in the wet season.

The FLC-EMS comprised two FLCs denoted as FLC1 and FLC2. FLC1 manages the battery charging and discharging, while FLC2 manages the DG operation. The FLC-EMS rules were designed based on expert knowledge and were used to schedule among the energy sources to meet the load demand while prioritizing renewable energy. The controller could switch at any time of operation, as required, to ensure an energy balance between the energy supply sources and the energy demand of the community. For this study, the membership functions of the variables and the FLC rules are constructed based on the operators' knowledge; however, in future work, the parameters of the membership functions can be tuned using PSO or any other optimization algorithm, and the fuzzy rules can be chosen based on the optimization algorithm.

Results from this study can be used as a general overview and a quick feasibility study to determine the technical and economic implications of implementing and operating HRES in off-grid rural communities in Nigeria.

# References


[1] Stears Data and Sterling, "Nigeria's State of Power 'Electrifying the Nation's economy,'" 2022.

[2] "Nigeria to Improve Electricity Access and Services to Citizens." https://www.worldbank.org/en/news/press-release/2021/02/05/nigeria-to-improve-electricity-access-and-services-to-citizens (accessed Jun. 28, 2022).

[3] "Nigeria - Living Standards Survey 2018-2019." https://microdata.worldbank.org/index.php/catalog/3827 (accessed Jan. 28, 2023).

[4] "Electric Power Sector Reform Act," *The Federal Government Press, Lagos, Nigeria*, 2005. https://rea.gov.ng/wp-content/uploads/2017/09/Electric-Power-Sector-Reform-Act-2005.pdf (accessed Jan. 29, 2023).

[5] K. Owebor, E. O. Diemuodeke, T. A. Briggs, and M. Imran, "Power Situation and renewable energy potentials in Nigeria – A case for integrated multi-generation technology," *Renew. Energy*, vol. 177, pp. 773–796, Nov. 2021, doi: 10.1016/J.RENENE.2021.06.017.

[6] A. P. Team and O. of the V. President, "Nigeria Power Baseline Report."

[7] "The Challenges with transforming the Nigerian power landscape,." https://www.pwc.com/ng/en/assets/pdf/power-roundtable-2016.pdf (accessed Jan. 28, 2023).

[8] "Population Estimates and Projections | Data Catalog," *Nigeria Population 2021*. https://datacatalog.worldbank.org/search/dataset/0037655/Population-Estimates-and-Projections (accessed Jan. 29, 2023).

[9] N. Enterprise Agency, "Solar Report Nigeria Commissioned by the Netherlands Enterprise Agency".

[10] P. E. Akhator, A. I. Obanor, and E. G. Sadjere, "Electricity situation and potential development in Nigeria using off-grid green energy solutions," *J. Appl. Sci. Environ. Manag.*, vol. 23, no. 3, p. 527, Apr. 2019, doi: 10.4314/JASEM.V23I3.24.

[11] ESMAP, "Global Photovoltaic Power Potential by Country.," *World Bank, Washington, DC.*, 2020.

[12] I. Ikeagwuani, O. Bamisile, S. Abbasoglu, and A. Julius, "Performance Comparison of PV and Wind Farm in Four Different Regions of Nigeria.," in *1ST ASUP UNWANA NATIONAL CONFERENCE*, 2016.

[13] M. Shaaban and J. O. Petinrin, "Renewable energy potentials in Nigeria: Meeting rural energy needs," *Renew. Sustain. Energy Rev.*, vol. 29, pp. 72–84, 2014, doi: 10.1016/J.RSER.2013.08.078.

[14] "World Energy Outlook 2014 – Analysis - IEA." https://www.iea.org/reports/world-energy-outlook-2014 (accessed Jan. 29, 2023).

[15] E.-I. Relations, "Renewable Energy: Global Challenges", Accessed: Jan. 18, 2023. [Online]. Available: https://www.e-ir.info/2016/05/27/renewable-energy-global-challenges/

[16] H. Farzaneh, "Design of a Hybrid Renewable Energy System Based on Supercritical Water Gasification of Biomass for Off-Grid Power Supply in Fukushima," *Energies*, vol. 12, no. 14. 2019. doi: 10.3390/en12142708.

[17] A. Shaqour, H. Farzaneh, Y. Yoshida, and T. Hinokuma, "Power control and simulation of a building integrated stand-alone hybrid PV-wind-battery system in Kasuga City, Japan,"

*Energy Reports*, vol. 6, pp. 1528–1544, Nov. 2020, doi: 10.1016/J.EGYR.2020.06.003.

[18] Z. Liu, H. Li, K. Liu, H. Yu, and K. Cheng, "Design of high-performance water-in-glass evacuated tube solar water heaters by a high-throughput screening based on machine learning: A combined modeling and experimental study," *Sol. Energy*, vol. 142, pp. 61–67, Jan. 2017, doi: 10.1016/J.SOLENER.2016.12.015.

[19] H. Farzaneh, "Energy Systems Modeling," *Energy Syst. Model.*, 2019, doi: 10.1007/978-981-13-6221-7.

[20] S. Pelland, D. Turcotte, G. Colgate, and A. Swingler, "Nemiah valley photovoltaic-diesel mini-grid: System performance and fuel saving based on one year of monitored data," *IEEE Trans. Sustain. Energy*, vol. 3, no. 1, pp. 167–175, Jan. 2012, doi: 10.1109/TSTE.2011.2170444.

[21] C. Yin, H. Wu, F. Locment, and M. Sechilariu, "Energy management of DC microgrid based on photovoltaic combined with diesel generator and supercapacitor," *Energy Convers. Manag.*, vol. 132, pp. 14–27, Jan. 2017, doi: 10.1016/j.enconman.2016.11.018.

[22] L. Xu, Z. Wang, Y. Liu, and L. Xing, "Energy allocation strategy based on fuzzy control considering optimal decision boundaries of standalone hybrid energy systems," *J. Clean. Prod.*, vol. 279, Jan. 2021, doi: 10.1016/J.JCLEPRO.2020.123810.

[23] J. Lian, Y. Zhang, C. Ma, Y. Yang, and E. Chaima, "A review on recent sizing methodologies of hybrid renewable energy systems," *Energy Convers. Manag.*, vol. 199, p. 112027, Nov. 2019, doi: 10.1016/J.ENCONMAN.2019.112027.

[24] K. Anoune, M. Bouya, A. Astito, and A. Ben Abdellah, "Sizing methods and optimization techniques for PV-wind based hybrid renewable energy system: A review," *Renew. Sustain. Energy Rev.*, vol. 93, pp. 652–673, Oct. 2018, doi: 10.1016/J.RSER.2018.05.032.

[25] Z. Liu, Y. Chen, R. Zhuo, and H. Jia, "Energy storage capacity optimization for autonomy microgrid considering CHP and EV scheduling," *Appl. Energy*, vol. 210, pp. 1113–1125, Jan. 2018, doi: 10.1016/J.APENERGY.2017.07.002.

[26] M. Amer, A. Namaane, and N. K. M'Sirdi, "Optimization of hybrid renewable energy systems (HRES) using PSO for cost reduction," *Energy Procedia*, vol. 42, pp. 318–327, 2013, doi: 10.1016/J.EGYPRO.2013.11.032.

[27] Y. Yoshida and H. Farzaneh, "Optimal design of a stand-alone residential hybrid microgrid system for enhancing renewable energy deployment in Japan," *Energies*, vol. 13, no. 7, Apr. 2020, doi: 10.3390/EN13071737.

[28] O. H. Mohammed, Y. Amirat, and M. Benbouzid, "Particle Swarm Optimization Of a Hybrid Wind/Tidal/PV/Battery Energy System. Application To a Remote Area In Bretagne, France," *Energy Procedia*, vol. 162, pp. 87–96, Apr. 2019, doi: 10.1016/J.EGYPRO.2019.04.010.

[29] Y. Yuan, T. Zhang, B. Shen, X. Yan, and T. Long, "A fuzzy logic energy management strategy for a photovoltaic/diesel/battery hybrid ship based on experimental database," *Energies*, vol. 11, no. 9, 2018, doi: 10.3390/EN11092211.

[30] M. Althubaiti, M. Bernard, and P. Musilek, "Fuzzy logic controller for hybrid renewable energy system with multiple types of storage," *Can. Conf. Electr. Comput. Eng.*, Jun. 2017, doi: 10.1109/CCECE.2017.7946738.

[31] A. Chaurey and T. C. Kandpal, "A techno-economic comparison of rural electrification based on solar home systems and PV microgrids," *Energy Policy 2010, Vol. 38, Pages 3118-3129*, vol. 38, no. 6, pp. 3118–3129, Jun. 2010, doi: 10.1016/J.ENPOL.2010.01.052.

[32] "[PDF] TECHNO ECONOMIC ANALYSIS OF STAND-ALONE HYBRID

RENEWABLE ENERGY SYSTEM HANIEH BORHANAZAD RESEARCH PROJECT SUBMITTED IN PARTIAL FULFILLMENT OF THE REQUIREMENTS FOR THE DEGREE OF MASTER OF ENGINEERING FACULTY OF ENGINEERING UNIVERSITY OF MALAYA | Semantic Scholar." https://www.semanticscholar.org/paper/TECHNO-ECONOMIC-ANALYSIS-OF-STAND-ALONE-HYBRID-IN-Lumpur./d9965017849575104ddde7ee4adbe8ef8dd31f7d (accessed Jan. 18, 2023).

[33] T. Hinokuma, H. Farzaneh, and A. Shaqour, "Techno-economic analysis of a fuzzy logic control based hybrid renewable energy system to power a university campus in Japan," *Energies*, vol. 14, no. 7, Apr. 2021, doi: 10.3390/EN14071960.

[34] S. Berrazouane and K. Mohammedi, "Parameter optimization via cuckoo optimization algorithm of fuzzy controller for energy management of a hybrid power system," *Energy Convers. Manag.*, vol. 78, pp. 652–660, Feb. 2014, doi: 10.1016/J.ENCONMAN.2013.11.018.

[35] W. M. Amutha and V. Rajini, "Cost benefit and technical analysis of rural electrification alternatives in southern India using HOMER," *Renew. Sustain. Energy Rev.*, vol. 62, pp. 236–246, Sep. 2016, doi: 10.1016/J.RSER.2016.04.042.

[36] M. A. Mohamed, A. M. Eltamaly, and A. I. Alolah, "Sizing and techno-economic analysis of stand-alone hybrid photovoltaic/wind/diesel/battery power generation systems," *J. Renew. Sustain. Energy*, vol. 7, no. 6, p. 063128, Dec. 2015, doi: 10.1063/1.4938154.

[37] J. Kennedy, R. Eberhart, and bls gov, "Particle Swarm Optimization".

[38] A. A. Moghaddam, A. Seifi, T. Niknam, and M. R. Alizadeh Pahlavani, "Multi-objective operation management of a renewable MG (micro-grid) with back-up micro-turbine/fuel cell/battery hybrid power source," *Energy*, vol. 36, no. 11, pp. 6490–6507, 2011, doi: 10.1016/J.ENERGY.2011.09.017.

[39] A. Kashefi Kaviani, G. H. Riahy, and S. M. Kouhsari, "Optimal design of a reliable hydrogen-based stand-alone wind/PV generating system, considering component outages," *Renew. Energy*, vol. 34, no. 11, pp. 2380–2390, Nov. 2009, doi: 10.1016/J.RENENE.2009.03.020.

[40] R. Johnston, "Fuzzy logic control," *Microelectronics J.*, vol. 26, no. 5, pp. 481–495, 1995, doi: 10.1016/0026-2692(95)98950-V.

[41] J. A. Goguen, "L. A. Zadeh. Fuzzy sets. Information and control, vol. 8 (1965), pp. 338–353. - L. A. Zadeh. Similarity relations and fuzzy orderings. Information sciences, vol. 3 (1971), pp. 177–200.," *J. Symb. Log.*, vol. 38, no. 4, pp. 656–657, Dec. 1973, doi: 10.2307/2272014.

[42] Y. Bai and D. Wang, "Fundamentals of fuzzy logic control — fuzzy sets, fuzzy rules and defuzzifications," *Adv. Ind. Control*, no. 9781846284687, pp. 17–36, 2006, doi: 10.1007/978-1-84628-469-4_2.

[43] "sun | power VR L Valve regulated lead-acid batteries for cyclic applications", Accessed: Jan. 18, 2023. [Online]. Available: www.hoppecke.com

[44] A. Hiendro, R. Kurnianto, M. Rajagukguk, Y. M. Simanjuntak, and Junaidi, "Techno-economic analysis of photovoltaic/wind hybrid system for onshore/remote area in Indonesia," *Energy*, vol. 59, pp. 652–657, Sep. 2013, doi: 10.1016/J.ENERGY.2013.06.005.

[45] C. L. Azimoh, P. Klintenberg, F. Wallin, B. Karlsson, and C. Mbohwa, "Electricity for development: Mini-grid solution for rural electrification in South Africa," *Energy Convers.*

*Manag.*, vol. 110, pp. 268–277, Feb. 2016, doi: 10.1016/J.ENCONMAN.2015.12.015.

[46] E. I. Come Zebra, H. J. van der Windt, G. Nhumaio, and A. P. C. Faaij, "A review of hybrid renewable energy systems in mini-grids for off-grid electrification in developing countries," *Renew. Sustain. Energy Rev.*, vol. 144, Jul. 2021, doi: 10.1016/J.RSER.2021.111036.